

# Alpha-Beta HMM: Hidden Markov Model Filtering with Equal Exit Probabilities and a Step-Size Parameter

Dongyan Sui, *Student Member, IEEE*, Haotian Pu, Siyang Leng, *Member, IEEE* and Stefan Vlaski, *Member, IEEE*

**Abstract**—The hidden Markov model (HMM) provides a powerful framework for inference in time-varying environments, where the underlying state evolves according to a Markov chain. To address the optimal filtering problem in general dynamic settings, we propose the  $\alpha\beta$ -HMM algorithm, which simplifies the state transition model to a Markov chain with equal exit probabilities and introduces a step-size parameter to balance the influence of observational data and the model. By analyzing the algorithm's dynamics in stationary environments, we uncover a fundamental trade-off between inference accuracy and adaptation capability, highlighting how key parameters and observation quality impact performance. A comprehensive theoretical analysis of the nonlinear dynamical system governing the evolution of the log-belief ratio, along with supporting numerical experiments, demonstrates that the proposed approach effectively balances adaptability and inference performance in dynamic environments.

**Index Terms**—Adaptive filters, Bayesian inference, Filtering algorithms, Hidden Markov models, Nonlinear dynamical systems

## I. INTRODUCTION

WE consider the Bayesian filtering problem, where a sensor provides noisy observations or signals  $\xi_i$  of the evolving state at each time step  $i = 1, 2, \dots$ . The aim is to estimate the underlying true state  $\theta_i^*$  at each time instant  $i$  given the observations  $\xi_1, \dots, \xi_i$ . This setup has numerous practical applications, including online speech recognition, tracking the kinematic state of a moving target (e.g., a car) from noisy observations, and performing online inference based on trained machine learning models.

This work was conducted while D.S. was a visiting PhD student at Imperial College London with support from the China Scholarship Council (No. 202406100217). S.L. was supported by the National Natural Science Foundation of China (No. 12471457). (Corresponding author: Siyang Leng)

Dongyan Sui is with College of Intelligent Robotics and Advanced Manufacturing, Fudan University, Shanghai 200433, China (e-mail: dysui22@m.fudan.edu.cn).

Haotian Pu is with Research Institute of Intelligent Complex Systems, Fudan University, Shanghai 200433, China (e-mail: htpu20@fudan.edu.cn).

Siyang Leng is with College of Intelligent Robotics and Advanced Manufacturing and Research Institute of Intelligent Complex Systems, Fudan University, Shanghai 200433, China (e-mail: syleng@fudan.edu.cn).

Stefan Vlaski is with Department of Electrical and Electronic Engineering, Imperial College London, UK (e-mail: s.vlaski@imperial.ac.uk).

For simplicity, we assume that the true state  $\theta_i^*$  belongs to a discrete set of  $M$  possible states  $\Theta = \{\theta_0, \theta_1, \dots, \theta_{M-1}\}$ . At each time step  $i$ , we assign to every state  $\theta \in \Theta$  a belief  $\mu_i(\theta)$ , which characterizes the confidence that  $\theta$  is the underlying true state at time  $i$  based on previous observations, i.e.,

$$\mu_i(\theta) = \mathbb{P}[\theta_i^* = \theta | \xi_1, \dots, \xi_i], \quad \theta \in \Theta. \quad (1)$$

Correct learning is said to occur at time  $i$  if the belief  $\mu_i(\theta)$  is maximized at the true state  $\theta = \theta_i^*$ . Conditioned on  $\theta_i^*$ , the observations  $\xi_i$  are independent and identically distributed (i.i.d.) over time  $i$ , take values in the space  $\Xi$ , and follow the probability density function  $f(\cdot | \theta_i^*)$ . The observation model, which specifies the likelihood of an observation  $\xi$  for each possible state  $\theta \in \Theta$  is denoted by

$$L(\xi | \theta), \quad \xi \in \Xi. \quad (2)$$

Viewed as a function of  $\xi$ ,  $L(\xi | \theta)$  can be either a probability density function or a probability mass function, depending on whether  $\xi$  is continuous or discrete. To ensure that the underlying true state can be successfully learned, we impose the following typical assumptions:

**Assumption 1 (Finiteness of KL Divergence):** For each pair of distinct states  $\theta$  and  $\theta'$ , the Kullback–Leibler (KL) divergence [1] between  $L(\xi | \theta)$  and  $L(\xi | \theta')$  satisfies:

$$D_{KL}(L(\xi | \theta) || L(\xi | \theta')) < \infty. \quad (3)$$

This assumption avoids trivial cases where a likelihood function model for a certain state completely dominates.

**Assumption 2 (Identifiability of the Underlying True State):**

$$\{\theta_i^*\} = \Theta_i^* = \arg \min_{\theta \in \Theta} D_{KL}(f(\cdot | \theta_i^*) || L(\cdot | \theta)). \quad (4)$$

Assumption 2 ensures that the underlying true state is the single best match for the observations under the likelihood model, which guarantees that successful learning can be achieved using observation model and data.

## A. Proposed Filtering Algorithm

In the proposed filtering algorithm, the belief vector  $\mu_i(\cdot)$  at each time instance  $i$  is updated from the previous belief  $\mu_{i-1}(\cdot)$  using the current environmental observation  $\xi_i \in \Xi$ .

For dynamic environments, we propose the following update rule:

$$\boldsymbol{\mu}_i(\theta_m) = \frac{[(1 - \alpha M) \boldsymbol{\mu}_{i-1}(\theta_m) + \alpha] L^\beta(\boldsymbol{\xi}_i|\theta_m)}{\sum_{n=0}^{M-1} [(1 - \alpha M) \boldsymbol{\mu}_{i-1}(\theta_n) + \alpha] L^\beta(\boldsymbol{\xi}_i|\theta_n)}, \quad (5)$$

where  $\alpha \in (0, 1/M)$  controls the weight assigned to the prior belief. Intuitively,  $\alpha$  can be interpreted as the exit probability — the probability that the underlying state transitions to a different value between two consecutive time instants (see Sec. IB for the formal definition). and  $\beta > 0$  is a step-size parameter. In the sequel we will demonstrate that this algorithm, referred to as  $\alpha\beta$ -HMM filtering, exhibits favorable learning performance in dynamic environments. We further elucidate the motivation behind this belief update rule, which can be interpreted as a simplified and generalized version of the hidden Markov model for online filtering.

### B. Interpretation of $\alpha\beta$ -HMM

In a static environment, where the underlying true state remains constant over time, the exact belief (1) can be computed exactly and recursively using Bayes' theorem, resulting in the following update rule for each possible state indexed by  $m$ :

$$\boldsymbol{\mu}_i(\theta_m) = \frac{\boldsymbol{\mu}_{i-1}(\theta_m)L(\boldsymbol{\xi}_i|\theta_m)}{\sum_{n=0}^{M-1} \boldsymbol{\mu}_{i-1}(\theta_n)L(\boldsymbol{\xi}_i|\theta_n)}. \quad (6)$$

Such constructions are widely applied in decision-making, learning, and inference tasks for single or multi-agent systems in static environments. In multi-agent networks or social networks, the sequential process where agents infer the true state by observing the decisions of peers and signals generated by the environment, is referred to as (non-)Bayesian social learning [2]–[10]. These models are widely used in economics, political science, and sociology to model the behavior of financial markets, social groups, and social networks [11], [12].

In dynamic environments, where the true state evolves over time, the reliance of (6) on past observations can make it less effective. In such scenarios, optimal filtering methods include the Kalman filter [13] and the hidden Markov filter [14]. The Kalman filter assumes that the state transitions of the environment follow a linear Gaussian model, while the hidden Markov filter assumes that the evolution of the true state follows a Markov chain. In this paper, we focus on filtering models related to the hidden Markov framework. Assuming that the transition probability matrix of the Markov chain between the  $M$  states at each iteration is denoted as  $P = [p_{nm}]_{M \times M}$ , where  $p_{nm} = \mathbb{P}[\theta_i^* = \theta_m | \theta_{i-1}^* = \theta_n]$ , then the optimal belief update, based on the hidden Markov model (HMM), is given by:

$$\boldsymbol{\mu}_i(\theta_m) = \frac{\sum_{n=0}^{M-1} p_{nm} \boldsymbol{\mu}_{i-1}(\theta_n) L(\boldsymbol{\xi}_i|\theta_m)}{\sum_{l=0}^{M-1} \sum_{n=0}^{M-1} p_{nl} \boldsymbol{\mu}_{i-1}(\theta_n) L(\boldsymbol{\xi}_i|\theta_l)}. \quad (7)$$

Observe that the optimal belief update under a hidden Markov model involves the entries of the full state transition matrix  $P$ . In practice,  $P$  is frequently unknown and challenging to estimate. In this work, we will instead study a simplified

HMM-based update, which is derived under the assumption of equal exit probabilities for state transitions. Specifically, the true state transitions with a probability  $h$ , and when a transition occurs, the next state is chosen uniformly at random. Under these assumptions, the transition probability matrix simplifies to:

$$p_{mn} = \begin{cases} 1 - h, & m = n, \\ \frac{h}{M-1}, & m \neq n. \end{cases} \quad (8)$$

This transforms the traditional HMM belief update into:

$$\boldsymbol{\mu}_i(\theta_m) = \frac{[(1 - \alpha M) \boldsymbol{\mu}_{i-1}(\theta_m) + \alpha] L(\boldsymbol{\xi}_i|\theta_m)}{\sum_{n=0}^{M-1} [(1 - \alpha M) \boldsymbol{\mu}_{i-1}(\theta_n) + \alpha] L(\boldsymbol{\xi}_i|\theta_n)}, \quad (9)$$

where  $\alpha = \frac{h}{M-1}$  represents the exit probability. It can be seen this formulation is a special case of (5) under the choice  $\beta = 1$ . Of course, for a general state transition matrix  $P$ , the simplified update rule (9) will be suboptimal compared to the optimal HMM filter (7). The advantage, on the other hand, is that (9) relies only on a single parameter  $\alpha$  that quantifies the volatility of the underlying true state. Indeed, examining (9), we observe that  $\alpha$  essentially controls the amount of weight placed on prior beliefs compared to the most recent observation. Note that when  $\alpha = 0$ , the above iteration degenerates into the classical Bayesian update (6). In this paper, since we focus on filtering in dynamic environments, we only consider the case where  $0 < h < 1$  and consequently,  $\alpha > 0$ .

By definition, in a more volatile environment, the value of  $\alpha$  should be higher, indicating a greater likelihood of state transitions. Conversely, in a relatively stable environment,  $\alpha$  should be smaller, indicating that the system is more likely to remain in the current state. In particular, when  $\alpha = 1/M$ , Eq. (9) reduces to:

$$\boldsymbol{\mu}_i(\theta_m) = \frac{L(\boldsymbol{\xi}_i|\theta_m)}{\sum_{n=0}^{M-1} L(\boldsymbol{\xi}_i|\theta_n)}. \quad (10)$$

In this case, the filter completely loses memory of past observations and relies solely on the current observation for learning.

The additional step-size parameter  $\beta$  in (5) is introduced to modulate the influence of the observation relative to memory. Intuitively, in a noisier environment where the observational noise is significant, the value of  $\beta$  should be smaller to mitigate the impact of noise. In this paper, we analyze the steady-state behavior of the  $\alpha\beta$ -HMM algorithm (5) and quantify the trade-off between learning and adaptability introduced by the hyperparameters  $\alpha$  and  $\beta$ . Numerical experiments validate our theoretical findings and highlight the practical effectiveness of the  $\alpha\beta$ -HMM in dynamic environments.

### C. Related Work

The hidden Markov model, proposed in the late 1960s [15], remains widely used due to its ease of implementation, ability to handle sequential data, and capacity to process inputs of variable lengths, making it suitable for numerous real-life applications [16]. Applications of HMMs are extensively studied in fields such as speech recognition [17]–[19], human activity recognition [20]–[22], and data analysis [23].

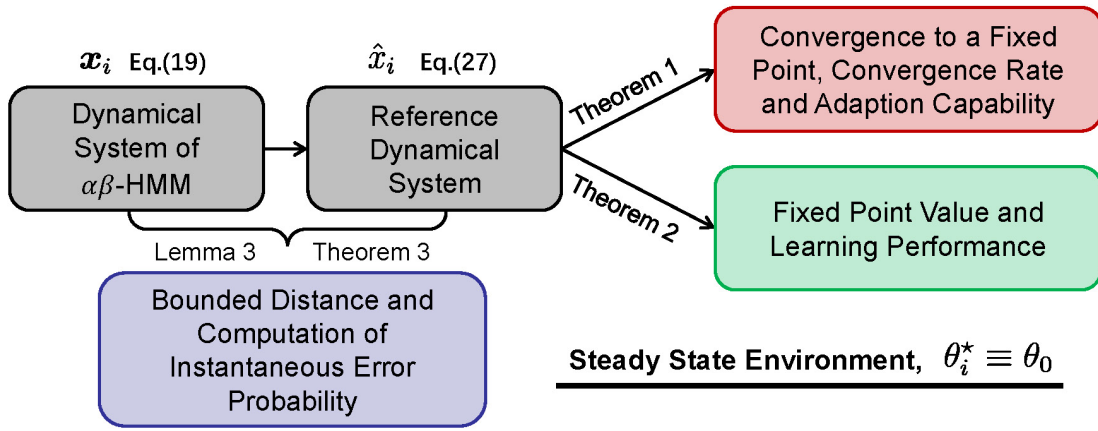


Fig. 1: Overview of the results presented in this work.

Theoretical studies on the dynamical analysis of HMMs often focus on the stability of the algorithm, particularly the conditions under which a wrongly initialized belief converges to the true posterior distribution. Filter stability, as discussed in [24], arises through two primary mechanisms: the ergodicity of the transition model [25], [26] and the informativeness of the observations [27].

The ergodicity of the transition model, which has been more extensively studied, is often analyzed through the Dobrushin coefficient. The Dobrushin coefficient maps the transition probabilities of the Markov chain to a real number in the interval  $[0, 1]$  and determines how quickly the HMM filter forgets its initial conditions and converges to the stationary distribution. In [26], a novel sufficient condition for the exponential stability of HMMs is proposed, leveraging Dobrushin coefficients associated with both the transition kernel and the informativeness of the observations.

In this work, we adopt a dynamical systems perspective, utilizing concepts such as fixed points to analyze the stochastic and deterministic dynamics of an HMM with equal exit probabilities. The ergodicity of the transition model can be easily adjusted by tuning the exit probability parameter  $\alpha$ , and the informativeness of the observations is incorporated through an identifiability parameter  $\underline{d}$ , which we formally define in Eq. (45) further below.

The online filtering problem has also been extensively studied in distributed settings. The adaptive social learning (ASL) strategy introduced in [28] is a linear model based on the logarithmic likelihood ratio of beliefs. ASL provides strong analytical guarantees and exhibits effective learning and adaptability in dynamic environments. Building on this framework, [9] implements multi-agent collaborative online machine learning. A distributed HMM framework for multi-agent systems was proposed in [29], enabling agents to collaboratively track dynamic states governed by Markov chains. Furthermore, [30] evaluates the performance of ASL by modeling the true state as a rare transition Markov chain.

#### D. Notation

Throughout this paper, we use  $i$  to denote time index, bold notation to represent random objects, while  $\mathbb{P}[\cdot]$ ,  $\mathbb{E}[\cdot]$

and  $\text{Var}[\cdot]$  represent the probability, expectation and variance operators, respectively. Inequalities between vectors are element-wise. Specifically, if  $v = [v_1, \dots, v_N]^\top$  and  $u = [u_1, \dots, u_N]^\top$ , then

$$v \geq u \Leftrightarrow v_i \geq u_i, \forall i = 1, \dots, N. \quad (11)$$

Functions of vectors are also applied element-wise. For example,

$$\exp(v) = [\exp(v_1), \dots, \exp(v_N)]^\top. \quad (12)$$

We denote the  $L_p$ -norm of a vector by  $\|\cdot\|_p$ , i.e.,

$$\|v\|_p = \left( \sum_{i=1}^N |v_i|^p \right)^{1/p}, \quad (13)$$

where  $v = [v_1, \dots, v_N]^\top$ ,  $0 < p < \infty$ , and

$$\|v\|_\infty = \max_{i=1, \dots, N} |v_i|. \quad (14)$$

We use  $0_N$  and  $1_N$  to denote the  $N$ -dimensional column vectors with all elements equal to 0 and 1, respectively.

#### E. Preview of Results

In this paper, we study the dynamical system underlying the evolution of the  $\alpha\beta$ -HMM and analyze its learning and adaptation performance. Due to the nonlinearity and stochasticity of the dynamical system corresponding to the  $\alpha\beta$ -HMM, we first introduce a deterministic reference dynamical system. Using the Contraction Mapping Theorem [31], we prove that in a steady state environment, the reference dynamical system converges to a fixed point and derive the convergence rate (Theorem 1). This result allows us to analyze the adaptability of the  $\alpha\beta$ -HMM and its dependence on parameters including the exit probability  $\alpha$ , step-size parameter  $\beta$  and the informativeness of observations. Subsequently, we calculate the position of the fixed point (Theorem 2) to analyze the learning performance of the  $\alpha\beta$ -HMM and its sensitivity to parameters. Finally, we prove that the distance between the original dynamical system and the reference system can be bounded, and by leveraging the fixed point of the reference system, we provide an upper bound for the instantaneous error probability of the algorithm (Theorem 3), thereby identifying

factors that influence the error probability. The flow of the argument is summarized in Fig. 1.

Unlike standard HMM filtering, the proposed  $\alpha\beta$ -HMM algorithm depends on only two scalars. Setting  $(\alpha, \beta) = (0, 1)$  recovers the classical Bayesian update, and a first-order linearization reproduces the ASL recursion [28]. Other choices of  $(\alpha, \beta)$  enable more granular control of the adaptation-performance trade-off in dynamic settings. For general choices  $(\alpha, \beta)$ , the  $\alpha\beta$ -HMM algorithm is non-linear, requiring adaptations in the analytical techniques compared to previous works. Numerical experiments in a wide range of non-stationary settings show that the inherent nonlinearity of the  $\alpha\beta$ -HMM yields consistently higher accuracy than (log-)linear algorithms such as the Bayesian formulation (6) and ASL [28].

## II. STEADY STATE DYNAMICAL ANALYSIS

While we motivated the  $\alpha\beta$ -HMM algorithm from a Markov chain with equal exit probabilities, we are interested in understanding its learning dynamics in a broader range of settings with potentially time-varying states. To this end, we will begin by quantifying in detail the ability of the  $\alpha\beta$ -HMM algorithm to identify the underlying state of the environment when it remains constant for an extended period of time. We will then proceed to characterize the adaptation capabilities of the algorithm when the environment does make a sudden change. Thus, without loss of generality, we assume that the underlying true state is  $\theta_0 \in \Theta$ , i.e.  $\theta_i^* = \theta_0$  for all  $i = 1, 2, \dots$ . We aim to analyze the dynamics of the log-likelihood ratio of the belief on wrong and true states, i.e.:

$$\mathbf{x}_{m,i} \triangleq \log \frac{\boldsymbol{\mu}_i(\theta_m)}{\boldsymbol{\mu}_i(\theta_0)}, \quad m = 1, \dots, M-1, \quad i = 0, 1, \dots \quad (15)$$

We refer to  $\mathbf{x}_{m,i}$  as the log-belief ratio. Using (5), the log-belief ratio evolves as:

$$\begin{aligned} & \log \frac{\boldsymbol{\mu}_i(\theta_m)}{\boldsymbol{\mu}_i(\theta_0)} \\ &= \log \frac{(1 - \alpha M)\boldsymbol{\mu}_{i-1}(\theta_m) + \alpha}{(1 - \alpha M)\boldsymbol{\mu}_{i-1}(\theta_0) + \alpha} + \beta \log \frac{L(\boldsymbol{\xi}_i|\theta_m)}{L(\boldsymbol{\xi}_i|\theta_0)}. \end{aligned} \quad (16)$$

The above dynamical system is both *nonlinear* and *stochastic*—*nonlinear* since the first term of the r.h.s. is nonlinear with respect to  $\log(\boldsymbol{\mu}_{i-1}(\theta_m)/\boldsymbol{\mu}_{i-1}(\theta_0))$  and *stochastic* since the system is driven by the function of a random process  $\boldsymbol{\xi}_i$ .

We first characterize the nonlinear mapping of the log-belief ratio from one time-instance to the next. From Eq. (5), we have  $\sum_{m=0}^{M-1} \boldsymbol{\mu}_i(\theta_m) = 1$ , for all  $i = 0, 1, \dots$ . Utilizing this

property, we can expand:

$$\begin{aligned} & \log \frac{(1 - \alpha M)\boldsymbol{\mu}_{i-1}(\theta_m) + \alpha}{(1 - \alpha M)\boldsymbol{\mu}_{i-1}(\theta_0) + \alpha} \\ &= \log \frac{(1 - \alpha M)\boldsymbol{\mu}_{i-1}(\theta_m) + \alpha \sum_{n=0}^{M-1} \boldsymbol{\mu}_{i-1}(\theta_n)}{(1 - \alpha M)\boldsymbol{\mu}_{i-1}(\theta_0) + \alpha \sum_{n=0}^{M-1} \boldsymbol{\mu}_{i-1}(\theta_n)} \\ &= \log \frac{(1 - \alpha M) \frac{\boldsymbol{\mu}_{i-1}(\theta_m)}{\boldsymbol{\mu}_{i-1}(\theta_0)} + \alpha + \alpha \sum_{n=1}^{M-1} \frac{\boldsymbol{\mu}_{i-1}(\theta_n)}{\boldsymbol{\mu}_{i-1}(\theta_0)}}{1 - \alpha M + \alpha + \alpha \sum_{n=1}^{M-1} \frac{\boldsymbol{\mu}_{i-1}(\theta_n)}{\boldsymbol{\mu}_{i-1}(\theta_0)}}} \\ &= \log \frac{(1 - \alpha M) \exp(\mathbf{x}_{m,i-1}) + \alpha + \alpha \sum_{n=1}^{M-1} \exp(\mathbf{x}_{n,i-1})}{1 - \alpha M + \alpha + \alpha \sum_{n=1}^{M-1} \exp(\mathbf{x}_{n,i-1})}. \end{aligned} \quad (17)$$

Defining:

$$\begin{aligned} & F_m(\mathbf{x}_1, \dots, \mathbf{x}_{M-1}) \triangleq \\ & \log \frac{(1 - \alpha M) \exp(\mathbf{x}_m) + \alpha + \alpha \sum_{n=1}^{M-1} \exp(\mathbf{x}_n)}{1 - \alpha M + \alpha + \alpha \sum_{n=1}^{M-1} \exp(\mathbf{x}_n)}, \end{aligned} \quad (18)$$

the dynamics for all  $m = 1, \dots, M-1$  and  $i = 1, 2, \dots$  can be expressed compactly as:

$$\mathbf{x}_{m,i} = F_m(\mathbf{x}_{1,i-1}, \dots, \mathbf{x}_{M-1,i-1}) + \beta \log \frac{L(\boldsymbol{\xi}_i|\theta_m)}{L(\boldsymbol{\xi}_i|\theta_0)}. \quad (19)$$

Now we will move on to the stochastic part. The second term on the r.h.s. of (19) satisfies that for all  $m = 1, \dots, M-1$ ,

$$\begin{aligned} & \mathbb{E} \left[ \log \frac{L(\boldsymbol{\xi}_i|\theta_m)}{L(\boldsymbol{\xi}_i|\theta_0)} \right] \\ &= \int_{\boldsymbol{\xi} \in \Xi} f(\boldsymbol{\xi}|\theta_0) \log \frac{L(\boldsymbol{\xi}|\theta_m)}{L(\boldsymbol{\xi}|\theta_0)} d\boldsymbol{\xi} \\ &= \int_{\boldsymbol{\xi} \in \Xi} f(\boldsymbol{\xi}|\theta_0) \log \frac{f(\boldsymbol{\xi}|\theta_0)}{L(\boldsymbol{\xi}|\theta_0)} d\boldsymbol{\xi} - \int_{\boldsymbol{\xi} \in \Xi} f(\boldsymbol{\xi}|\theta_0) \log \frac{f(\boldsymbol{\xi}|\theta_0)}{L(\boldsymbol{\xi}|\theta_m)} d\boldsymbol{\xi} \\ &= D_{\text{KL}}(f(\cdot|\theta_0)||L(\cdot|\theta_0)) - D_{\text{KL}}(f(\cdot|\theta_0)||L(\cdot|\theta_m)) \\ &\triangleq -d_m < 0. \end{aligned} \quad (20)$$

The last inequality above is guaranteed by Assumption 2. From the definition of  $d_m$ , it is evident that it characterizes the filter's ability to distinguish any incorrect state  $\theta_m$  from the underlying true state  $\theta_0$  using the likelihood models  $L(\cdot|\theta_m)$  and the observation  $\boldsymbol{\xi}$ . A larger  $d_m$  indicates stronger identifiability. Define the identifiability vector

$$\mathbf{d} = [d_1, \dots, d_{M-1}]^\top, \quad (21)$$

the state vector

$$\mathbf{x}_i = [\mathbf{x}_{1,i}, \dots, \mathbf{x}_{M-1,i}]^\top, \quad (22)$$

and the mapping

$$F(\mathbf{x}) = [F_1(\mathbf{x}_1, \dots, \mathbf{x}_{M-1}), \dots, F_{M-1}(\mathbf{x}_1, \dots, \mathbf{x}_{M-1})]^\top. \quad (23)$$

Taking conditional expectations and rewriting in vector form, the dynamics in (19) become:

$$\mathbb{E}[\mathbf{x}_i|\mathbf{x}_{i-1}] = F(\mathbf{x}_{i-1}) - \beta \mathbf{d}. \quad (24)$$

Taking the expectation again, we derive the following dynamical system for the evolution of the expectation:

$$\mathbb{E}[\mathbf{x}_i] = \mathbb{E}[F(\mathbf{x}_{i-1})] - \beta \mathbf{d}. \quad (25)$$

Clearly, for a general nonlinear function  $F$ ,

$$\mathbb{E}[F(\mathbf{x})] \neq F(\mathbb{E}[\mathbf{x}]), \quad (26)$$

Nevertheless, relation (25) motivates the following  $(M-1)$ -dimensional deterministic dynamical system, referred to as the reference dynamical system. Subsequently, we will demonstrate that due to the contraction properties of the function  $F$ , the asymptotic difference between the stochastic system and this reference system can be bounded:

$$\hat{x}_i = F(\hat{x}_{i-1}) - \beta d. \quad (27)$$

Here  $\hat{x}_i$  is deterministic and acts as the counterpart of the original stochastic log-belief ratio  $\mathbf{x}_i$ .

In the following theoretical analysis, we focus on the scenario where  $0 < \alpha < 1/M$ , ensuring  $0 < 1 - \alpha M < 1$ . This setting, referred to as slow-changing conditions, corresponds to the regime where past observations are likely to be informative of the current state and also facilitates a more analytically tractable analysis of the algorithm.

*Remark 1:* It is worth noting that for all  $m = 1, \dots, M-1$ ,

$$F_m(0, \dots, 0) = 0, \quad (28)$$

$$\left. \frac{\partial F_m}{\partial x_m} \right|_{(0, \dots, 0)} = 1 - \alpha M, \quad (29)$$

$$\left. \frac{\partial F_m}{\partial x_n} \right|_{(0, \dots, 0)} = 0, \quad \forall n \neq m. \quad (30)$$

By applying a multivariate Taylor expansion to  $F(x)$  around  $x = 0_{M-1}$  up to the first-order term, for all  $m = 1, \dots, M-1$  we have:

$$F_m(x_1, \dots, x_{M-1}) = (1 - \alpha M)x_m + o(\|x\|), \quad (31)$$

then we derive the linear approximation of the system (19), which is:

$$\mathbf{x}_{m,i} = (1 - \alpha M)\mathbf{x}_{m,i-1} + \beta \log \frac{L(\xi_i | \theta_m)}{L(\xi_i | \theta_0)}. \quad (32)$$

The above equation can be seen as a model that resembles the single-agent version of the Adaptive Social Learning model [28] in non-Bayesian social learning, which has the following dynamics for log-belief ratio:

$$\mathbf{x}_{m,i} = (1 - \delta)\mathbf{x}_{m,i-1} + \delta \log \frac{L(\xi_i | \theta_m)}{L(\xi_i | \theta_0)}, \quad (33)$$

where  $\delta$  is the step-size parameter. Equations (33) and (32) both apply a discount to the information from the previous time step during the iteration process. The subtle difference between them is that the former employs two independent parameters, where  $\alpha$  characterizes the rate of change of the environment, and  $\beta$  implements the tradeoff between memory and new information. As remarked earlier, this added flexibility is useful because the choice  $\beta = 1$  recovers the optimal HMM-filter for a Markov chain with equal exit probability. Setting  $\alpha = \frac{\delta}{M}$ ,  $\beta = \delta$  instead yields adaptive social learning variant from [28]. We will illustrate in the numerical results how different parameter choices can yield improved performance in specific settings.

## A. Convergence Rate and Adaption Ability

In this part, we will prove that the reference dynamical system (27) will converge to a fixed point at an exponential rate. Based on this, we can analyze the adaptation capability and how it can be influenced by the exit probability  $\alpha$ , step-size parameter  $\beta$  and identifiability vector  $d$  defined in (21).

*Definition 1 (Contraction):* Let  $(X, \rho)$  be a metric space. A mapping  $T : X \rightarrow X$  is a contraction, if there exists a constant  $c$ , with  $0 \leq c < 1$ , such that

$$\rho(T(x), T(y)) \leq c\rho(x, y) \quad (34)$$

for all  $x, y \in X$ .

Based on the above definition, we now present the following lemma, which demonstrates that the mapping  $F(x)$  defined in (23) is a contraction on the non-positive region; this property facilitates the convergence analysis of the reference dynamical system.

*Lemma 1:* Consider  $0 < \alpha < 1/M$  and  $\beta > 0$ , the mapping  $F$  defined in (23) and (18) has the following properties:

- 1)  $F((-\infty, 0]^{M-1}) \subset (-\infty, 0]^{M-1}$ ; that is,  $F$  maps the non-positive region into itself.
- 2)  $F$  is a contraction on  $(-\infty, 0]^{M-1}$  with respect to the  $L_\infty$ -norm.

*Proof:* Appendix I. ■

Let  $T : X \rightarrow X$  be a mapping. A point of  $x \in X$  such that

$$T(x) = x \quad (35)$$

is called a fixed point of  $X$ . For a discrete dynamical system  $x_i = T(x_{i-1})$ , a fixed point of the map  $T$  corresponds to an equilibrium state of the system. In the remainder of this paper, we will consistently refer to it as the fixed point.

For the reference dynamical system (27), its fixed point has the following property:

*Lemma 2:* The fixed point  $\hat{x}^\infty$  of the reference dynamical system (27) satisfies:

$$\hat{x}^\infty = [\hat{x}_1^\infty, \dots, \hat{x}_{M-1}^\infty]^\top, \quad (36)$$

$$\hat{x}_m^\infty = \log \frac{\alpha}{\alpha \exp(\beta d_m) + (1 - \alpha M)(\exp(\beta d_m) - 1)\hat{\mu}_0^\infty}, \quad (37)$$

where

$$\hat{\mu}_0^\infty = \frac{1}{1 + \sum_{m=1}^{M-1} \exp(\hat{x}_m^\infty)}. \quad (38)$$

*Proof:* Supplementary Material I. ■

Lemma 2 shows that the reference dynamical system has a fixed point, which is strictly negative for all components. To verify this, for all  $m = 1, \dots, M-1$ , when  $1 - \alpha M > 0$  we have:

$$\alpha \exp(\beta d_m) + (1 - \alpha M)(\exp(\beta d_m) - 1)\hat{\mu}_0^\infty > \alpha \exp(\beta d_m), \quad (39)$$

implying

$$\hat{x}_m^\infty < -\beta d_m < 0. \quad (40)$$

This result implies that the reference dynamical system learns correctly, since the log-belief ratio  $\hat{x}_{m,i}$  is strictly less than zero for any wrong state  $\theta_m$ . When  $1 - \alpha M > 0$ , increasing either  $\beta$  (the weight assigned to the observational data) or  $d_m$

(the distinguishability between  $\theta_0$  and  $\theta_m$ ) drives the fixed-point value  $\hat{x}_m^\infty$  further negative, indicating stronger confidence in the true state relative to the competing state  $\theta_m$ .

Now we are able to provide the main result regarding the convergence of the reference dynamical system (27) and its convergence rate.

*Theorem 1:* When  $0 < \alpha < 1/M$  and  $\beta > 0$ ,  $\hat{x}_i$  defined in (27) will converge to a unique fixed point, i.e.,

$$\lim_{i \rightarrow \infty} \hat{x}_i = \hat{x}^\infty, \quad (41)$$

and

$$\|\hat{x}_i - \hat{x}^\infty\|_\infty \leq \lambda \|\hat{x}_{i-1} - \hat{x}^\infty\|_\infty, \quad (42)$$

where

$$\lambda = 1 - \min \left\{ \frac{2\alpha}{1 - \alpha M + 2\alpha}, \frac{\beta \underline{d}}{\bar{x}_0 - \log \frac{\alpha}{1 - \alpha M + \alpha} + \beta \underline{d}} \right\}, \quad (43)$$

$$\bar{x}_0 = \max \left\{ \{\hat{x}_{m,0}\}_{m=1}^{M-1}, 0 \right\}, \quad (44)$$

and

$$\underline{d} = \min_{m=1, \dots, M-1} d_m. \quad (45)$$

*Proof:* Appendix II ■

*Remark 2:* Theorem 1 provides an upper bound on the convergence rate of  $\hat{x}_i$  to  $\hat{x}^\infty$  in the sense of the  $L_\infty$ -norm, which decreases as the exit probability  $\alpha$  increases, as shown in (43). We can also observe the impact of the data, captured in  $\beta \underline{d}$ , and the initial setting, captured in  $\bar{x}_0$ , on the convergence rate of the reference dynamical system to its fixed point. The parameter  $\underline{d}$  depends on both the local likelihood function (e.g., pre-trained models) and the quality of observations (e.g., variance of local data noise). This parameter, referred to as the *identifiability parameter*, reflects the ability to distinguish between the two most challenging states. From Theorem 1, it follows that higher identifiability  $\underline{d}$  and higher  $\beta$  accelerate the convergence to the fixed point, while the deviation in the initial setting, captured in  $\bar{x}_0$ , slows down the convergence rate.

The impact of the exit probability  $\alpha$ , step-size  $\beta$  and the identifiability parameter  $\underline{d}$  on the convergence rate are further illustrated by the following corollary.

*Corollary 1:* When  $0 < \alpha < 1/M$  and  $\beta > 0$ , the convergence rate of the reference dynamical system is characterized by the following inequality, which further reveals the influence of the identifiability parameter  $\underline{d}$ :

$$\|\exp(\hat{x}_i) - \exp(\hat{x}^\infty)\|_1 \leq \gamma \|\exp(\hat{x}_{i-1}) - \exp(\hat{x}^\infty)\|_1, \quad (46)$$

where

$$\gamma = \frac{(1 - \alpha M)(1 + 2\alpha U(M - 1))}{(1 - \alpha M + \alpha)^2} \exp(-\beta \underline{d}), \quad (47)$$

$$U = \max \left\{ 1, \{\exp(\hat{x}_{m,0})\}_{m=1}^{M-1} \right\}, \quad (48)$$

$$\underline{d} = \min_{m=1, \dots, M-1} d_m. \quad (49)$$

Furthermore, if the initial value of the reference dynamical system satisfies:

$$\hat{x}_0 \geq \hat{x}^\infty, \quad (50)$$

then a more precise bound of the contraction rate can be given by:

$$\|\exp(\hat{x}_i) - \exp(\hat{x}^\infty)\|_1 \leq \gamma_1 \|\exp(\hat{x}_{i-1}) - \exp(\hat{x}^\infty)\|_1, \quad (51)$$

where

$$\gamma_1 = \frac{\exp(-\beta \underline{d})(1 - \alpha M)}{(1 - \alpha M + \alpha)^2}. \quad (52)$$

*Proof:* Supplementary Material II. ■

Corollary 1 provides a more precise upper bound on the convergence rate of the reference dynamical system to its fixed point. It shows that as  $\alpha \rightarrow 1/M$ , the contraction coefficient  $\gamma \rightarrow 0$ , indicating that the rate of convergence accelerates. This observation aligns with intuition: when  $\alpha \rightarrow 1/M$  in equation (5), the system relies less on historical observations and becomes more reliant on the most recently observed data. In subsequent numerical experiments, we observe that, generally larger values of  $\alpha < 1/M$  lead to faster convergence. Additionally, as  $\beta \rightarrow \infty$ ,  $\gamma \rightarrow 0$ , which shows that increasing the value of  $\beta$  leads to a faster convergence rate of the system to its fixed point.

When the components of the initial values of the reference dynamical system satisfy certain consistency conditions, a more precise upper bound on the convergence rate can be provided. It is worth noting that when the algorithm adopts a uniform prior belief distribution:

$$\mu_0(\theta_m) = \mu_0(\theta_n), \quad \forall \theta_m, \theta_n \in \Theta, \quad (53)$$

we have  $\hat{x}_0 = 0_{M-1}$ . The initial condition (50), will therefore be satisfied. This condition reflects an unbiased prior belief, which aligns with typical requirements in practical algorithmic settings.

*Remark 3:* The convergence rate of the reference dynamical system to its fixed point, as presented in Theorem 1, plays a crucial role in understanding the *adaptation capabilities* of the algorithm. Specifically, when the environment remains in a fixed state for an extended period, the reference dynamical system converges to its fixed point at an exponential rate. When the environment state changes, the corresponding fixed point shifts accordingly, and the system will converge to the new fixed point exponentially fast, as illustrated in Fig. 2. The convergence speed depends on the choice of the parameters  $\alpha$  and  $\beta$ , and the quality of the data and model. When using the traditional Bayesian update (6), as indicated by equations (17) and (27) with  $\alpha = 0$  and  $\beta = 1$ , the corresponding deterministic dynamical system simplifies to the linear equation

$$\hat{x}_i = \hat{x}_{i-1} - d, \quad (54)$$

which shows that the log-belief ratio evolves linearly over time. This slower rate explains why the proposed algorithm exhibits superior adaptability in dynamic environments.

*Example 1:* To further illustrate the adaptability difference between  $\alpha\beta$ -HMM and the Bayesian update (6), consider a binary decision-making problem with candidate states,  $\theta_0$  and  $\theta_1$ . Before time instant  $T_1$ , the environmental signals are more aligned with the likelihood function corresponding to  $\theta_0$ , whereas after  $T_1$ , they become more aligned with the likelihood function corresponding to  $\theta_1$ .

We analyze the expected evolution of the log-belief ratio:

$$\mathbf{x}_i = \log \frac{\mu_i(\theta_1)}{\mu_i(\theta_0)}. \quad (55)$$

For the traditional Bayes' formula (6), we have:

$$\hat{x}_i = \hat{x}_{i-1} + \mathbb{E} \left[ \log \frac{L(\xi_i|\theta_1)}{L(\xi_i|\theta_0)} \right] = \begin{cases} \hat{x}_{i-1} - d_{s1} & \text{if } i \leq T_1, \\ \hat{x}_{i-1} + d_{s2} & \text{otherwise,} \end{cases} \quad (56)$$

where

$$d_{s1} = D_{\text{KL}}(f(\cdot|\theta_0)||L(\cdot|\theta_1)) - D_{\text{KL}}(f(\cdot|\theta_0)||L(\cdot|\theta_0)) > 0, \quad (57)$$

and

$$d_{s2} = D_{\text{KL}}(f(\cdot|\theta_1)||L(\cdot|\theta_0)) - D_{\text{KL}}(f(\cdot|\theta_1)||L(\cdot|\theta_1)) > 0. \quad (58)$$

Starting from an initial value  $\hat{x}_0$ ,  $\hat{x}_i$  will initially decrease linearly with time before  $T_1$  and then increases. Let  $T_{\text{adapt}}$  denote the time required for correcting past beliefs, that is, the time needed for adaptation to the new environment. Specifically,  $\hat{x}_i > 0$  when  $i > T_1 + T_{\text{adapt}}$ . For the Bayesian update(6), we have:

$$T_{\text{adapt}} > \frac{d_{s1}T_1 - \hat{x}_0}{d_{s2}}. \quad (59)$$

For  $\alpha\beta$ -HMM, we have:

$$\hat{x}_i = F(\hat{x}_{i-1}) + \beta \mathbb{E} \left[ \log \frac{L(\xi_i|\theta_1)}{L(\xi_i|\theta_0)} \right], \quad (60)$$

Following Theorem 1, we can see that:

$$|\hat{x}_{T_1} - \hat{x}_{s1}^\infty| \leq \lambda_{s1}^{T_1} |\hat{x}_0 - \hat{x}_{s1}^\infty|, \quad (61)$$

and when  $i > T_1$ ,

$$|\hat{x}_i - \hat{x}_{s2}^\infty| \leq \lambda_{s2}^{i-T_1} |\hat{x}_{T_1} - \hat{x}_{s2}^\infty|, \quad (62)$$

where  $\hat{x}_{s1}^\infty < 0$  and  $\hat{x}_{s2}^\infty > 0$  are the two fixed points before and after  $T_1$ , respectively, and  $\lambda_{s1}$  and  $\lambda_{s2}$  are the convergence coefficients in two stages defined as in Theorem 1.

The adaptation time  $T_{\text{adapt}}$  for  $\alpha\beta$ -HMM should satisfy:

$$\hat{x}_{T_1+T_{\text{adapt}}} > 0. \quad (63)$$

A sufficient condition for (63) is:

$$|\hat{x}_{T_1+T_{\text{adapt}}} - \hat{x}_{s2}^\infty| < |\hat{x}_{s2}^\infty|. \quad (64)$$

Following (61) and (62), we have for  $i > T_1$ ,

$$\begin{aligned} |\hat{x}_i - \hat{x}_{s2}^\infty| &\leq \lambda_{s2}^{i-T_1} |\hat{x}_{T_1} - \hat{x}_{s2}^\infty| \\ &\leq \lambda_{s2}^{i-T_1} (|\hat{x}_{T_1} - \hat{x}_{s1}^\infty| + |\hat{x}_{s2}^\infty - \hat{x}_{s1}^\infty|) \\ &\leq \lambda_{s2}^{i-T_1} \left( \lambda_{s1}^{T_1} |\hat{x}_0 - \hat{x}_{s1}^\infty| + |\hat{x}_{s2}^\infty - \hat{x}_{s1}^\infty| \right). \end{aligned} \quad (65)$$

To guarantee (64), it is sufficient that:

$$\lambda_{s2}^{T_{\text{adapt}}} \left( \lambda_{s1}^{T_1} |\hat{x}_0 - \hat{x}_{s1}^\infty| + |\hat{x}_{s2}^\infty - \hat{x}_{s1}^\infty| \right) < |\hat{x}_{s2}^\infty|, \quad (66)$$

which implies

$$T_{\text{adapt}} > \frac{\log \frac{|\hat{x}_{s2}^\infty|}{\lambda_{s1}^{T_1} |\hat{x}_0 - \hat{x}_{s1}^\infty| + |\hat{x}_{s2}^\infty - \hat{x}_{s1}^\infty|}}{\log \lambda_{s2}}. \quad (67)$$

Comparing (59) and (67), it can be observed that in Bayes' formula (6), the adaptation time increases linearly with  $T_1$ , and is highly dependent on the initial value  $\hat{x}_0$ . In contrast, under the  $\alpha\beta$ -HMM strategy, the influence of the initial value  $\hat{x}_0$  vanishes as  $T_1$  approaches infinity. Furthermore, since  $\lambda_{s1} < 1$ , the adaptation time will not increase indefinitely with  $T_1$ , but instead will stabilize at a certain value. It is worth noting that, under similar settings, [28] also derives an adaptation time in the case of a single agent, which also exhibits the independence of the previous stationary interval  $T_1$  when it is sufficiently large. Figure 2 presents a comparison of the adaptability of Bayes' formula and  $\alpha\beta$ -HMM under different  $T_1$  values in this example.

## B. Fixed Point Value and Learning Performance

In this section, we quantify the learning performance of the  $\alpha\beta$ -HMM and examine its dependence on the exit probability  $\alpha$ , the step-size parameter  $\beta$ , and the identifiability parameter  $\underline{d}$ . Since we have already proven that the reference dynamical system converges to the unique fixed point as described in Lemma 2, the position of the fixed point will be sufficient to characterize the resulting learning performance. Due to the nonlinearity of (37), explicitly solving for the exact fixed point value is challenging. Nevertheless, we can provide an estimate of its value. In Theorem 2, we derive upper and lower bounds for the counterpart of the belief  $\mu_i(\cdot)$  in the reference dynamical system.

Given that

$$\mathbf{x}_{m,i} = \log \frac{\mu_i(\theta_m)}{\mu_i(\theta_0)}, \quad (68)$$

we can obtain

$$\mu_i(\theta_m) = \begin{cases} 1 / \left( 1 + \sum_{m=1}^{M-1} \exp(\mathbf{x}_{m,i}) \right), & m = 0, \\ \exp(\mathbf{x}_{m,i}) / \left( 1 + \sum_{m=1}^{M-1} \exp(\mathbf{x}_{m,i}) \right), & m \neq 0. \end{cases} \quad (69)$$

Since  $\hat{x}_{m,i}$  can be seen as the counterpart of  $\mathbf{x}_{m,i}$  in reference dynamical system, similarly we can define

$$\hat{\mu}_i(\theta_m) = \begin{cases} 1 / \left( 1 + \sum_{m=1}^{M-1} \exp(\hat{x}_{m,i}) \right), & m = 0, \\ \exp(\hat{x}_{m,i}) / \left( 1 + \sum_{m=1}^{M-1} \exp(\hat{x}_{m,i}) \right), & m \neq 0, \end{cases} \quad (70)$$

and then

$$\hat{x}_{m,i} = \log \frac{\hat{\mu}_i(\theta_m)}{\hat{\mu}_i(\theta_0)}, \quad (71)$$

for all  $m = 1, \dots, M-1$  and  $i = 0, 1, \dots$ . Here  $\hat{\mu}_i(\theta)$  can be seen as the counterpart of belief on state  $\theta$  in the reference dynamical system. By Theorem 1 and basic limit properties,

$$\lim_{i \rightarrow \infty} \hat{\mu}_i(\theta_m) = \hat{\mu}_m^\infty, \quad \forall m = 0, \dots, M-1, \quad (72)$$

where

$$\hat{\mu}_m^\infty = \begin{cases} 1 / \left( 1 + \sum_{m=1}^{M-1} \exp(\hat{x}_m^\infty) \right), & m = 0, \\ \exp(\hat{x}_m^\infty) / \left( 1 + \sum_{m=1}^{M-1} \exp(\hat{x}_m^\infty) \right), & m \neq 0. \end{cases} \quad (73)$$

The value of  $\hat{\mu}_0^\infty$ , which represents the steady-state belief on the true state in reference dynamical system, reflects the learning performance of the algorithm: the closer  $\hat{\mu}_0^\infty$  is to 1,

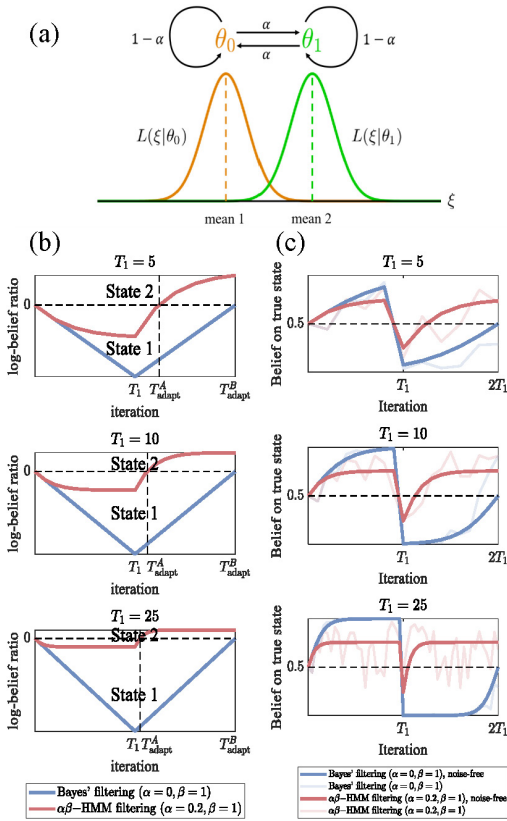


Fig. 2: (a) Two candidate states are considered,  $\theta_0$ (state 1) and  $\theta_1$ (state 2), where the likelihood models for these two states, as well as the model for environmental observations under these two states, are both standard normal density functions with distinct means. The environment remains in state 1 until time  $T_1$ , after which it switches to state 2 for the remaining duration. (b) The log-belief ratio  $\log(\mu_i(\theta_1)/\mu_i(\theta_0))$  is compared over time for both the  $\alpha\beta$ -HMM and the traditional Bayes' filter (6). Here  $T_{\text{adapt}}^A$  and  $T_{\text{adapt}}^B$  represent the adaptation time required for the  $\alpha\beta$ -HMM and Bayes' formula, respectively. The  $\alpha\beta$ -HMM filter quickly converges and stabilizes at the fixed point, whereas the Bayes' filter continues to accumulate "confidence" in the current state. When the environment changes, the Bayes' filter must counteract the previously accumulated confidence and adjust at a slower, linear rate. This slower adjustment prevents the Bayes' filter from rapidly responding to changes in the true state. The difference in adaptability between the two algorithms is particularly pronounced when  $T_1$  is large. (c) The belief on the true state under both algorithms over time. In deterministic expected dynamics, the  $\alpha\beta$ -HMM exhibits superior adaptability, with the belief remaining above 0.5 for most of the time, indicating correct decision-making. When observation noise is present, the  $\alpha\beta$ -HMM algorithm exhibits larger fluctuations to maintain adaptability. This trade-off allows the  $\alpha\beta$ -HMM to remain responsive, albeit at the cost of increased variance in belief estimates.

the better the distinction between correct and incorrect states at steady state; conversely, the closer  $\hat{\mu}_0^\infty$  is to  $1/M$ , the more ambiguous the learning outcome. We provide upper and lower bound estimates for  $\hat{\mu}_0^\infty$  in the following theorem.

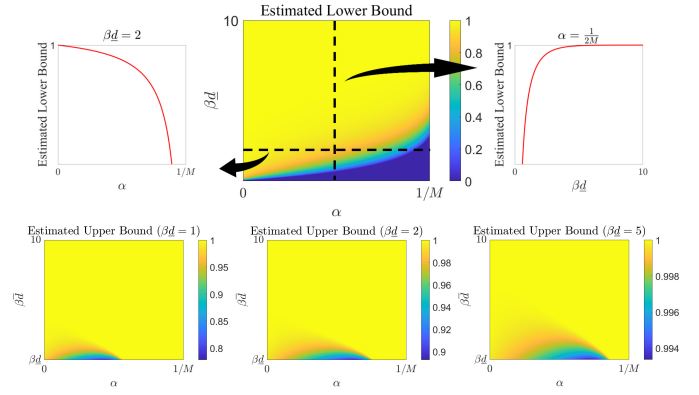


Fig. 3: The visualizations of the upper and lower bounds given in Theorem 2 as functions of the parameters  $\alpha$ ,  $\beta\bar{d}$ , and  $\beta\bar{d}$ . Top: Visualization of the lower bound function. The left and right subplots show how the lower bound varies with one parameter while the other is fixed, with  $\alpha$  and  $\beta\bar{d}$  set to specific values in each case. Bottom: Visualization of the upper bound function. Since the upper bound is a function of  $\alpha$ ,  $\beta\bar{d}$ , and  $\beta\bar{d}$  (where  $\bar{d} > \underline{d}$ ), the three subplots illustrate how the upper bound varies with  $\alpha$  and  $\beta\bar{d}$  for different fixed values of  $\beta\bar{d}$ .

*Theorem 2:* When  $0 < \alpha < 1/M$ ,  $\beta > 0$ , and the underlying true state remains unchanged, the  $\hat{\mu}_0^\infty$  defined in (73) satisfies the following bounds:

$$\hat{\mu}_0^\infty \geq \frac{(1 - \alpha M) \exp(\beta\bar{d}) - 1 + \alpha}{(1 - \alpha M)(\exp(\beta\bar{d}) - 1)} \triangleq \underline{\mu}, \quad (74)$$

$$\hat{\mu}_0^\infty \leq \frac{(1 - \alpha M - \alpha + \alpha/\underline{\mu}) \exp(\beta\bar{d}) - 1 + \alpha}{(1 - \alpha M)(\exp(\beta\bar{d}) - 1)} \triangleq \bar{\mu}, \quad (75)$$

where

$$\underline{d} = \min_{m=1, \dots, M-1} d_m, \quad (76)$$

and

$$\bar{d} = \max_{m=1, \dots, M-1} d_m. \quad (77)$$

*Proof:* Appendix III ■

*Remark 4:* The upper and lower bounds in Theorem 2, as functions of the parameters  $\alpha$ ,  $\beta\bar{d}$ , and  $\beta\bar{d}$ , are illustrated in Figure 3. We observe that when  $\alpha$  is smaller and  $\beta\bar{d}$  is larger, the steady-state belief on the correct state in the reference dynamical system is higher, indicating improved learning performance. This observation aligns with intuition: better learning performance is expected in less volatile environments, with lower observation noise, and a more accurate local likelihood model. The step-size parameter  $\beta$  and the identifiability parameter  $\underline{d}$  play a decisive role; when either  $\beta$  or  $\underline{d}$  is large, good learning performance is ensured in deterministic dynamical system, noise-free by construction, even when  $\alpha$  is relatively large. This means that, in the deterministic setting, accurate inference is possible in volatile environments, provided that the quality of the data model and observations is high enough or that the value of  $\beta$  is large enough. However, choosing a large  $\beta$  comes at the cost of amplifying the effect of observation noise, as we will further demonstrate in Section III.

### III. FROM DETERMINISTIC TO STOCHASTIC SYSTEMS

In this section, we discuss the relationship between the stochastic dynamical system induced by  $\alpha\beta$ -HMM, represented by (19), and the reference dynamical system (27), establishing that the dynamics of (27) are representative of the stochastic system (19), which describes the actual learning dynamics of the  $\alpha\beta$ -HMM recursion. In Lemma 3, we show that the expected distance between  $\mathbf{x}_i$  and the fixed point of the reference dynamical system can be asymptotically bounded. Then, in Theorem 3, we compute the instantaneous error probability of the  $\alpha\beta$ -HMM based on the fixed point of the reference dynamical system. To ensure tractability of the theoretical analysis, we introduce the following assumption.

*Assumption 3 (Bounded Log-Likelihood Ratio):* There exists a positive constant  $C$  such that:

$$\max_{m=1,\dots,M-1} \sup_{\xi \in \Xi} \left| \log \frac{L(\xi|\theta_m)}{L(\xi|\theta_0)} + d_m \right| \leq C, \quad a.s.. \quad (78)$$

Note that

$$\mathbb{E} \left[ \log \frac{L(\xi|\theta_m)}{L(\xi|\theta_0)} \right] = -d_m. \quad (79)$$

The Assumption 3 actually requires that the log-likelihood ratio can be almost surely bounded.

To compare the reference dynamical system and the original stochastic dynamical system, we recall the two recursions previously introduced:

- 1) The evolution of the log-belief ratio in  $\alpha\beta$ -HMM,  $\mathbf{x}_{m,i}$  ( $m = 1, \dots, M-1$ ):

$$\mathbf{x}_{m,i} = F_m(\mathbf{x}_{1,i-1}, \dots, \mathbf{x}_{M-1,i-1}) + \beta \log \frac{L(\xi_i|\theta_m)}{L(\xi_i|\theta_0)}. \quad (80)$$

- 2) The evolution of the counterpart of  $\mathbf{x}_{m,i}$  in the reference dynamical system,  $\hat{\mathbf{x}}_{m,i}$ :

$$\hat{\mathbf{x}}_{m,i} = F_m(\hat{\mathbf{x}}_{1,i-1}, \dots, \hat{\mathbf{x}}_{M-1,i-1}) - \beta d_m, \quad (81)$$

where it is established in Theorem 1 that  $\hat{\mathbf{x}}_{m,i} \rightarrow \hat{\mathbf{x}}_m^\infty$ , as  $i \rightarrow \infty$ .

The following lemma establishes the relationship between the two dynamical systems (80) and (81):

*Lemma 3:* Let  $\mathbf{x}_{m,i}$  and  $\hat{\mathbf{x}}_{m,i}$  follow the dynamical system in (80) and (81), respectively. Then, the following equation holds:

$$\mathbb{E} [\|\mathbf{x}_i - \hat{\mathbf{x}}^\infty\|_\infty] \leq O(\lambda_1^i) + \frac{\beta C}{1 - \lambda_1}, \quad (82)$$

where  $\hat{\mathbf{x}}^\infty$  is the fixed point of reference dynamical system (27),

$$\lambda_1 = 1 - \min \left\{ \frac{2\alpha}{1 - \alpha M + 2\alpha}, \frac{\beta \underline{d}}{2 \log \frac{1 - \alpha M + \alpha}{\alpha} + \beta C} \right\}, \quad (83)$$

with  $C$  and  $\underline{d}$  defined in (78) and (45), respectively.

*Proof:* Appendix IV ■

In Lemma 3, we show that the distance between the original dynamical system and the fixed point of the reference dynamical system can be bounded. The coefficient  $\lambda_1$  is always less than 1, then as the time instant approaches infinity, the upper

bound of the expected distance between the two is related to the first absolute moment of the log-likelihood ratio of the observational model and the contraction coefficient  $\lambda_1$ . In other words, when the observation noise decreases, the stochastic dynamical system corresponding to the  $\alpha\beta$ -HMM (80) approaches the fixed point of the reference dynamical system.

To evaluate the learning performance of  $\alpha\beta$ -HMM, we introduce an important metric: the *instantaneous error probability*:

$$p_i^e \triangleq \mathbb{P} [\exists \theta_m \neq \theta_0, \text{ s.t. } \boldsymbol{\mu}_i(\theta_m) \geq \boldsymbol{\mu}_i(\theta_0)]. \quad (84)$$

From this definition, it is clear that the instantaneous error probability quantifies the probability of failing to correctly identify the underlying true state at a given time  $i$  during the online filtering process. We will then provide an estimate of this metric in the steady-state scenario for the proposed  $\alpha\beta$ -HMM algorithm.

*Theorem 3:* When  $0 < \alpha < 1/M$ ,  $\beta > 0$ , and the underlying true state remains constant, i.e.  $\theta_i^* = \theta_0$  for all  $i = 1, 2, \dots$ , the instantaneous error probability for the  $\alpha\beta$ -HMM algorithm (5) satisfies:

$$p_i^e \leq \frac{O(\lambda_1^i) + \beta C}{-(1 - \lambda_1)\bar{x}^\infty}, \quad (85)$$

where

$$\bar{x}^\infty = \max_{m=1,\dots,M-1} \hat{x}_m^\infty < 0, \quad (86)$$

other variable definitions remain unchanged from those presented in Lemma 3. Furthermore, we have the following asymptotic estimate of the instantaneous error probability:

If  $\beta = O(\alpha)$ , then:

$$\lim_{\alpha \rightarrow 0} \left( \limsup_{i \rightarrow \infty} p_i^e \right) = 0. \quad (87)$$

*Proof:* Appendix V ■

*Remark 5:* The contraction coefficient  $\lambda_1$  in Theorem 3 is always less than 1, consequently the upper bound of the instantaneous error probability decays exponentially with time and eventually converges to a fixed value

$$\frac{\beta C}{-(1 - \lambda_1)\bar{x}^\infty}. \quad (88)$$

This result indicates that under the  $\alpha\beta$ -HMM framework, the probability of erroneous learning cannot be guaranteed to asymptotically approach zero for all choices of  $\alpha$  and  $\beta$ , even in steady-state conditions, which contrasts with the behavior predicted by Bayes' formula [8]. However, by sacrificing some learning performance, the  $\alpha\beta$ -HMM framework significantly enhances adaptability, as previously discussed. The steady-state error learning probability can be reduced either by (1) pushing the fixed point  $\hat{\mathbf{x}}^\infty$  of the deterministic system further away from zero and accelerating the convergence rate (i.e., reducing  $\lambda_1$ ), noting that, as shown in earlier analyses, improving the identifiability parameter  $\underline{d}$  facilitates this outcome, or by (2) reducing the observation noise, thereby increasing the informativeness of the observations.

The asymptotic analysis results for small  $\alpha$  further indicate that as  $\alpha$  approaches zero, the instantaneous error probability

diminishes over time. This phenomenon highlights the trade-off between the learning capability and the adaptation ability of the algorithm: while a small  $\alpha$  yields good learning performance, it reduces the adaptation rate, as illustrated in (83). Moreover, when  $\alpha = 0$ , the proposed algorithm degenerates into Bayes' formula, which, as discussed in Remark 3, exhibits poor adaptability.

#### IV. PARAMETER SELECTION AND TUNING

Based on the analysis in Section II, we summarize the impacts of the exit probability parameter  $\alpha$  and the step-size parameter  $\beta$  as follows:

- 1) The exit probability parameter  $\alpha$  can be employed to adjust the algorithm's adaptability and learning performance. In more volatile environments, a larger value of  $\alpha$  is preferred to enhance adaptability (Theorem 1). Conversely, if the goal is to ensure superior learning performance, a smaller value of  $\alpha$  should be selected (Theorems 2 and 3). This conclusion is consistent with intuition, since  $\alpha$  reflects the volatility of the environment.
- 2) The step-size parameter  $\beta$  serves to balance the algorithm's adaptability, learning performance, and the influence of observation noise. Specifically, under the assumption of the identifiability of the underlying true state (Assumption 2), a larger  $\beta$  results in a faster adaptation rate (Theorem 1, Corollary 1) and improved learning performance in noise-free scenarios (Theorem 2). However, since  $\beta$  also amplifies the effect of noise (Theorem 3), selecting a large  $\beta$  is beneficial when the observation noise is minimal, while in high-noise conditions a large  $\beta$  may lead to instability in the algorithm's performance. Notably, when  $\beta$  is set to 1, the proposed  $\alpha\beta$ -HMM algorithm can be interpreted as the HMM model corresponding to the equal exit probability transition matrix.

#### V. NUMERICAL EXPERIMENTS

##### A. Algorithm performance and parameter tuning

In the first numerical experiment, we consider a filtering task where the sensor provides noisy signals following a standard normal distribution. The number of possible states is set to  $M = 5$ , and the observations follow  $\xi_i \sim \mathcal{N}(\theta_i^*, \sigma^2)$ . The likelihood function model is given by  $L(\xi|\theta_m) = \mathcal{N}(\theta_m, \sigma^2)$ , where  $\theta_m = m + 1$ ,  $m = 0, \dots, M - 1$ . We assume that every ten iterations, the underlying true state,  $\theta_i^*$ , will be randomly reselected from the  $M$  possible states. Under this setting, the evolution of the true state does not strictly follow a Markov chain. As we show, the  $\alpha\beta$ -HMM algorithm nevertheless continues to yield meaningful performance.

Figure 4 compares the performance of the  $\alpha\beta$ -HMM algorithm with the algorithm employing linear log-belief ratio dynamics:

$$\mu_i(\theta_m) = \frac{\mu_{i-1}^{1-\alpha M}(\theta_m) L^\beta(\xi_i|\theta_m)}{\sum_{n=0}^{M-1} \mu_{i-1}^{1-\alpha M}(\theta_n) L^\beta(\xi_i|\theta_n)}, \quad (89)$$

referred to as the linearized  $\alpha\beta$ -HMM algorithm, under varying values of the parameter  $\alpha$ , while keeping  $\beta = 1$  in both algorithms to ensure a consistent influence of the data. It is noteworthy that the belief update rule in (89) exhibits similarities to the one presented in [28], as elaborated in Remark 1. From Figure 4, it can be observed that under various parameter settings, the accuracy of the  $\alpha\beta$ -HMM algorithm is no worse than that of the linearized algorithm, and its performance with respect to  $\alpha$  is more stable. A more pronounced advantage is observed when  $\alpha$  is small. These results highlight the benefits of the nonlinearity inherent in the  $\alpha\beta$ -HMM algorithm. Focusing solely on the  $\alpha\beta$ -HMM algorithm, when  $\alpha$  is relatively small (Fig. 4(c)), the algorithm struggles to track transitions between two similar underlying true states (e.g., at iteration 40, when the true state transitions from  $\theta_2$  to  $\theta_3$ , the algorithm fails to detect this change). However, as  $\alpha$  increases, as shown in Fig. 4(d), the belief in the current true state decreases, allowing the algorithm to better track transitions between similar states, though with some delay. When  $\alpha$  is further increased, as illustrated in Fig. 4(e), the algorithm quickly adapts to state transitions, demonstrating excellent adaptability. Nevertheless, due to the reduced confidence in the current true state, the algorithm becomes more sensitive to noise, leading to intermittent correct learning even during stable periods of the true state.

The influence of the step-size parameter  $\beta$  under different levels of observation noise is illustrated in Fig. 5. In the case of less noisy observations ( $\sigma^2 = 1$ ), a higher value of  $\beta$  leads to improved final learning accuracy across all three parameter settings. In contrast, when the observation noise is larger ( $\sigma^2 = 2$ ), the learning accuracy decreases as  $\beta$  increases. These experimental results are consistent with the theoretical findings presented in Theorem 3.

##### B. Trade-off between learning and adaption

The above results can be explained using the steady-state analysis results from Theorem 1 and Theorem 2. Assuming that  $\theta_i^*$  remains unchanged as  $\theta_0$ , i.e.,  $\theta_i^* \equiv \theta^*$ , it is straightforward to compute:

$$d_m = D_{\text{KL}}(L(\cdot|\theta^*)|L(\cdot|\theta_m)) = \frac{(l-m)^2}{2\sigma^2}, \quad \theta^* = \theta_l. \quad (90)$$

Thus, when  $\theta^*$  and  $\sigma^2$  are fixed, the value of  $d_m$  remains constant. In Fig. 6(a), we observe that increasing the value of  $\alpha$  while keeping  $\beta$  constant causes the fixed points of the reference dynamical system to approach zero, indicating lower confidence and higher sensitivity. At the same time, the convergence rate to the fixed point increases as  $\alpha$  approaches  $1/M$ . Conversely, when  $\alpha$  is fixed and  $\beta$  is adjusted, larger values of  $\beta$  lead to fixed points further from zero and faster convergence rates. These findings are consistent with the analytical results presented in Theorems 1 and 2.

In Fig. 6(b), we further compare the convergence rates of  $\hat{x}_{m,i}$  to the fixed point under different parameter settings when  $\theta_i^* \equiv \theta_0$ . The linear decay observed on the semilog Y-axis, the upper bound estimation, and the variation in convergence rate with respect to adjustments in parameters  $\alpha$  and  $\beta$  are all

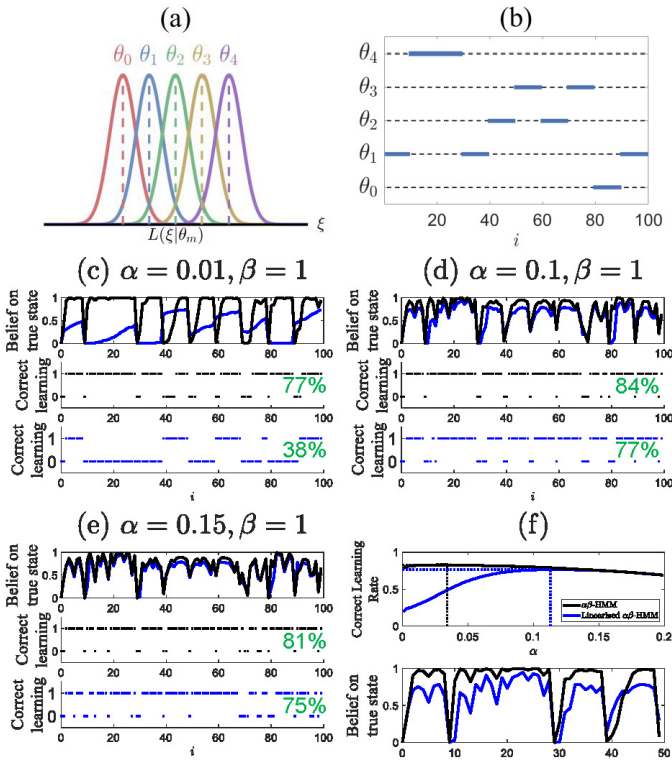


Fig. 4: (a) The likelihood model. (b) The underlying true state in each iteration. (c-e) Evolution of the belief on the true state for both  $\alpha\beta$ -HMM and linearized  $\alpha\beta$ -HMM under different values of  $\alpha$  with  $\beta = 1$  and  $\sigma = 0.5$  fixed. The success or failure of identification at different iterations is shown, i.e., whether the true state is assigned the highest belief. The black line represents the results for  $\alpha\beta$ -HMM, the blue line represents the results for linearized  $\alpha\beta$ -HMM, and the green numbers indicate the success rate of learning over 100 iterations. (f) Top: Learning rates for correctly identifying the true state of the two algorithms under various values of  $\alpha$ , evaluated via Monte Carlo simulation over 10,000 iterations. Bottom: Evolution of the belief on the true state for both algorithms under their optimal  $\alpha$  settings.

consistent with the conclusions of Theorem 1 and Corollary 1, which predict exponential convergence to the fixed point with a rate that increases with  $\alpha$  and  $\beta$ . In Fig.6(c), we demonstrate the evolution of the belief on the underlying true state  $\theta_0$  in the reference dynamical system, i.e.,  $\hat{\mu}_i(\theta_0)$ , under different parameter settings. It can be observed that as  $\alpha$  increases and  $\beta$  decreases, both the steady-state belief on the true state and its estimated lower bound gradually decline. Furthermore, as  $\alpha$  and  $\beta$  increase, the belief converges to the steady state more rapidly. These results align with the analysis in Theorem 1 and Theorem 2, emphasizing the trade-off between learning performance and adaptation capability through the tuning of  $\alpha$ , and highlighting the role of the step-size parameter  $\beta$  in shaping the convergence behavior.

### C. Error Probability of the algorithm

In this numerical experiment, we aim to validate the conclusion from Theorem 3 regarding the error probability of

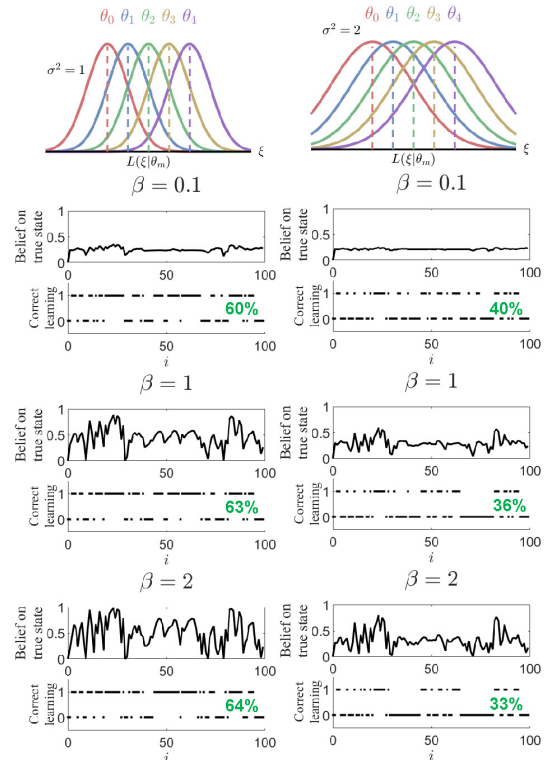


Fig. 5: Likelihood models for noise variances  $\sigma^2 = 1$  and  $\sigma^2 = 0.5$ , and the evolution of the belief on true state and the correct learning rate under different step-size parameter  $\beta$  settings.

$\alpha\beta$ -HMM. We assume there are three possible states,  $\Theta = \{\theta_0, \theta_1, \theta_2\}$ , with the underlying true state remaining constant as  $\theta_0$ . The observations  $\xi_i$  are assumed to follow a truncated normal distribution with a mean of 0, specifically  $\xi_i = \sigma \mathbf{W}_i$ , where  $\sigma$  is a positive constant and  $\mathbf{W}_i$  is truncated zero-mean Gaussian noise. The corresponding likelihood model under state  $\theta_m$  assumes the observations are given by  $L(\cdot|\theta_m) = m + 1 + \sigma \mathbf{W}_i$ . All random variables are truncated within the range  $[-5, 5]$ .

Fig. 7(a) shows the likelihood function  $L(\xi|\theta_m)$  for all  $\theta_m \in \Theta$  and the true distribution function of the observations  $f(\xi|\theta^*)$  under different  $\sigma$ , clearly the likelihood model of state  $\theta_0$  is closer to the true distribution. Note that there is no exact true state according to the likelihood model, as  $f$  is not equal to the likelihood function on any states.

Fig. 7(b) illustrates the time evolution of the instantaneous error probability defined in (84) under different parameter settings, which is estimated through 1,000 Monte Carlo simulations. A clear trend of decay over time is observed, consistent with the predictions of Theorem 3. Additionally, when  $\sigma$  is fixed and  $\beta = \alpha$ , increasing  $\alpha$  reduces the contraction coefficient  $\lambda_1$ , accelerating the convergence of the error probability. However, it also shifts the fixed point closer to zero, increasing the probability of error occurrence, as described in (85). Moreover, regardless of the value of  $\sigma$ , when  $\beta = \alpha$  is sufficiently small, the error probability always converges to zero over time. This observation is consistent with the asymptotic result described in (87). On the other hand,

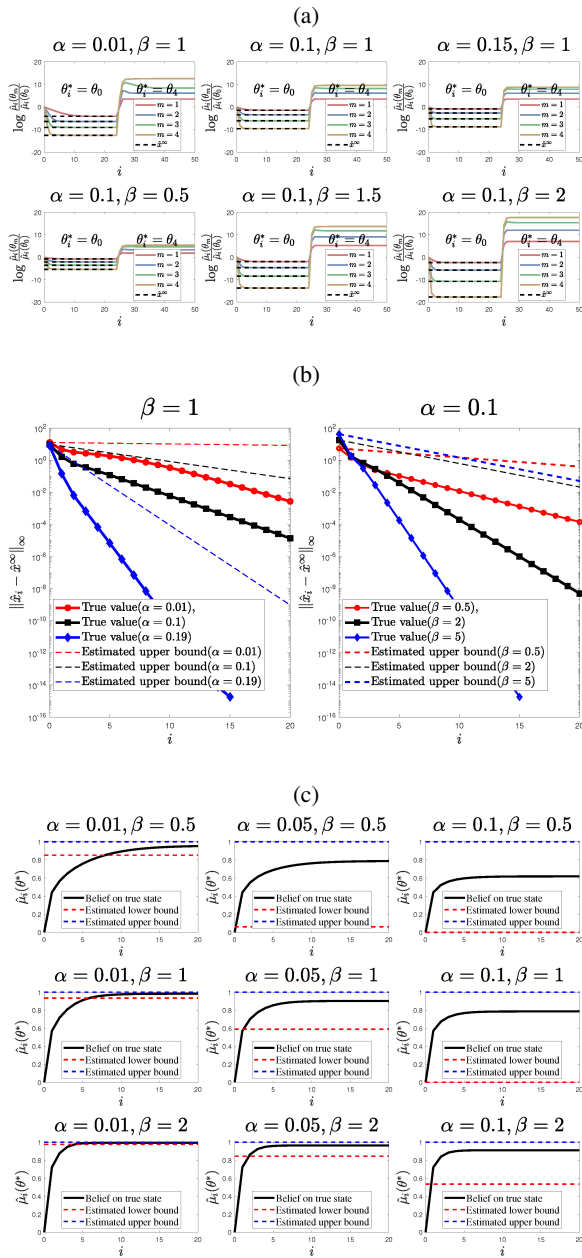


Fig. 6: (a) Comparison of the log-belief ratio evolution in the reference dynamical system under different parameter settings. Before iteration  $i = 25$ , the underlying true state is  $\theta_i^* = \theta_0$ , and after that,  $\theta_i^* = \theta_4$ . The fixed point,  $\hat{x}^\infty$ , is computed using (37) when  $\theta_i^* = \theta_0$ . (b) Comparison of the true evolution of  $\|\hat{x}_i - \hat{x}^\infty\|_\infty$  and the evolution estimated using the contraction coefficient  $\lambda$  in Theorem 1 on semilog y-axis coordinates. (c) Evolution of belief on the underlying true state in the reference dynamical system under different parameter settings. The estimated upper and lower bounds are computed using Theorem 2.

when  $\alpha$  and  $\beta$  are fixed, an increase in  $\sigma$  reduces the filter's ability to distinguish between states, leading to a smaller  $d_m$ . This results in a larger contraction coefficient  $\lambda_1$ , slowing the convergence of the error probability. Simultaneously, the fixed

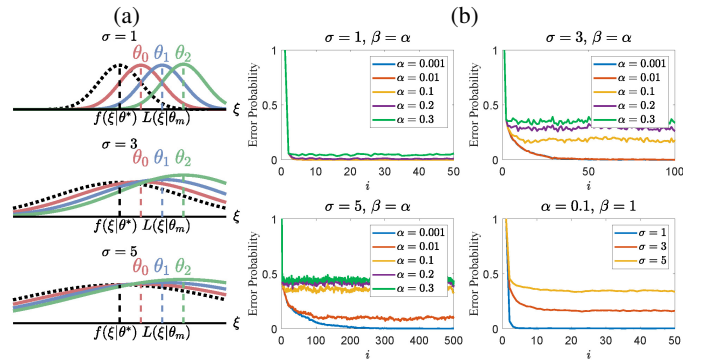


Fig. 7: (a) The likelihood function for all states and the true distribution function of the observations under different parameter settings. The dashed lines represent the true distribution functions of the observations, while the solid lines indicate the likelihood functions. (b) The evolution of the instantaneous error probability with iterations under different parameter settings.

point moves closer to zero, further increasing the probability of error occurrence. These observations further validate the theoretical analysis presented in Theorem 3.

## VI. CONCLUSION AND FUTURE WORK

In this paper, we studied the online optimal filtering problem by assuming that the environmental state follows a Markov chain with equal exit probability and proposed the  $\alpha\beta$ -HMM algorithm. By conducting a dynamical analysis of the discrete-time stochastic system associated with the algorithm and its deterministic counterpart under steady-state conditions, we investigated the influence of the exit probability  $\alpha$ , the step-size parameter  $\beta$  and the identifiability parameter  $\underline{d}$  on the algorithm's adaptability and learning performance.

Our findings reveal that a larger  $\alpha$  enhances convergence speed but lowers confidence in the correct state at the fixed point, increasing the likelihood of erroneous learning. Thus, the choice of  $\alpha$  embodies a tradeoff between adaptability and learning precision. When the underlying true state is identifiable, increasing the step-size parameter  $\beta$  enhances both learning and adaption performance, but it also amplifies observation noise and should therefore be moderated in high-noise scenarios. Conversely, higher identifiability—representing superior observation quality or a more accurate local model—accelerates convergence, improves adaptability, and shifts the fixed point further from zero, enhancing overall learning performance.

Our analytical approach leverages the contraction properties of nonlinear mappings, proving that the expected discrepancy between the deterministic reference dynamical system and the original stochastic dynamical system decays over time and remains bounded. This allows us to use the fixed point of the deterministic system to provide insights into the algorithm's instantaneous error probability.

This work lays the groundwork for extending hidden Markov filtering methods from single filter to multi-agent

systems. Future efforts will explore generalizations to multi-agent scenarios and examine the asymptotic performance of the  $\alpha\beta$ -HMM algorithm in environments with dynamic states.

### APPENDIX I PROOF OF LEMMA 1

For any non-positive input  $x \in (-\infty, 0]^{M-1}$ , we have  $\exp(x_m) \leq 1$  for  $m = 1, \dots, M-1$ . Consequently,

$$F_m(x) = \log \frac{(1 - \alpha M) \exp(x_m) + \alpha + \alpha \sum_{n=1}^{M-1} \exp(x_n)}{1 - \alpha M + \alpha + \alpha \sum_{n=1}^{M-1} \exp(x_n)} \leq 0, \quad (91)$$

so that  $F(x) \in (-\infty, 0]^{M-1}$ . For any  $x = [x_1, \dots, x_{M-1}]^\top$  and  $x' = [x'_1, \dots, x'_{M-1}]^\top$ , by Lagrange's main value theorem, we have:

$$F(x) - F(x') = J_F(c) (x - x'), \quad (92)$$

where  $J_F(c)$  is the Jacobian matrix of  $F$  at  $c = tx + (1-t)x'$  with  $t \in (0, 1)$ .

Due to the submultiplicative property of matrix norms:

$$\|F(x) - F(x')\|_\infty \leq \|J_F(c)\|_\infty \|x - x'\|_\infty. \quad (93)$$

The function  $F_m(x)$  is given by:

$$F_m(x) = \log \Lambda_m(x) - \log \Gamma(x), \quad (94)$$

where

$$\Lambda_m(x) = (1 - \alpha M) \exp(x_m) + \alpha + \alpha \sum_{n=1}^{M-1} \exp(x_n), \quad (95)$$

$$\Gamma(x) = 1 - \alpha M + \alpha + \alpha \sum_{n=1}^{M-1} \exp(x_n). \quad (96)$$

The partial derivative of  $F_m(x)$  with respect to  $x_\ell$  ( $\ell \neq m$ ) is:

$$\begin{aligned} \frac{\partial F_m}{\partial x_\ell}(x) &= \frac{\alpha \exp(x_\ell)}{\Lambda_m(x)} - \frac{\alpha \exp(x_\ell)}{\Gamma(x)} \\ &= \frac{\alpha(1 - \alpha M) \exp(x_\ell) (1 - \exp(x_m))}{\Lambda_m(x) \Gamma(x)}. \end{aligned} \quad (97)$$

Since  $0 < \alpha < 1/M$ ,  $\Lambda_m(x) > 0$  and  $\Gamma(x) > 0$ , we have:

$$\frac{\partial F_m}{\partial x_\ell}(x) \geq 0, \quad \text{if } x_m \leq 0. \quad (98)$$

Similarly, for all  $m = 1, \dots, M-1$ , we have:

$$\begin{aligned} \frac{\partial F_m}{\partial x_m}(x) &= \frac{(1 - \alpha M + \alpha) \exp(x_m)}{\Lambda_m(x)} - \frac{\alpha \exp(x_m)}{\Gamma(x)} \\ &= \frac{(1 - \alpha M) \exp(x_m) (\alpha + \Gamma(x) - \alpha \exp(x_m))}{\Lambda_m(x) \Gamma(x)}. \end{aligned} \quad (99)$$

Since  $\Gamma(x) > \alpha \exp(x_m)$  for all  $m$ , we have:

$$\frac{\partial F_m}{\partial x_m}(x) > 0. \quad (100)$$

Summing over  $l$ , the Jacobian satisfies:

$$\begin{aligned} \sum_{\ell=1}^{M-1} \frac{\partial F_m}{\partial x_\ell}(x) &= \frac{(1 - \alpha M) \exp(x_m) + \alpha \sum_{\ell=1}^{M-1} \exp(x_\ell)}{\Lambda_m(x)} \\ &\quad - \frac{\alpha \sum_{\ell=1}^{M-1} \exp(x_\ell)}{\Gamma(x)} \\ &= \frac{\Lambda_m(x) - \alpha}{\Lambda_m(x)} - \frac{\Gamma(x) - (1 - \alpha M + \alpha)}{\Gamma(x)} \\ &= \frac{1 - \alpha M + \alpha}{\Gamma(x)} - \frac{\alpha}{\Lambda_m(x)}. \end{aligned} \quad (101)$$

For further analysis, by substituting the  $\exp(x_m)$  with  $y_m$  in the r.h.s. of (101), we can define

$$H_m(y_1, \dots, y_{M-1}) \triangleq \frac{1 - \alpha M + \alpha}{1 - \alpha M + \alpha + \alpha \sum_{n=1}^{m-1} y_n} - \frac{1}{(1 - \alpha M) y_m + \alpha + \alpha \sum_{n=1}^{M-1} y_n}, \quad (102)$$

where  $y_m > 0$  for all  $m = 1, \dots, M-1$ . By differentiating with respect to  $y_m$ , it can be verified that:

$$\frac{\partial H_m}{\partial y_m} \geq 0, \quad \text{if } y_m \leq 1. \quad (103)$$

Hence when  $y_m \leq 1$ ,

$$\begin{aligned} H_m(y_1, \dots, y_{M-1}) &\leq H_m(y_1, \dots, y_{m-1}, 1, y_{m+1}, \dots, y_M) \\ &= \frac{1 - \alpha M}{1 - \alpha M + 2\alpha + \sum_{n \neq m}^{M-1} y_n} \\ &< \frac{1 - \alpha M}{1 - \alpha M + 2\alpha} < 1. \end{aligned} \quad (104)$$

Thus, for  $x_m \leq 0$ , we have  $\exp(x_m) \leq 1$ , leading to:

$$\sum_{\ell=1}^{M-1} \frac{\partial F_m}{\partial x_\ell}(x) < \frac{1 - \alpha M}{1 - \alpha M + 2\alpha}, \quad \text{if } x_m \leq 0. \quad (105)$$

For  $x, x' \in (-\infty, 0]$ ,  $c = tx + (1-t)x' \in (-\infty, 0]$ , and for all  $m, l = 1, \dots, M-1$ , we have:

$$[J_F(c)]_{ml} = \frac{\partial F_m}{\partial x_l}(c) \geq 0, \quad (106)$$

and

$$\begin{aligned} \|J_F(c)\|_\infty &= \max_{m=1, \dots, M-1} \sum_{l=1}^{M-1} \left| \frac{\partial F_m}{\partial x_l}(c) \right| \\ &= \max_{m=1, \dots, M-1} \sum_{l=1}^{M-1} \frac{\partial F_m}{\partial x_l}(c) \\ &< \frac{1 - \alpha M}{1 - \alpha M + 2\alpha}. \end{aligned} \quad (107)$$

Following (93) we obtain:

$$\|F(x) - F(x')\|_\infty \leq \frac{1 - \alpha M}{1 - \alpha M + 2\alpha} \|x - x'\|_\infty, \quad (108)$$

which completes the proof of Lemma 1.

**APPENDIX II**  
**PROOF OF THEOREM 1**

We first show that regardless of the initial value  $\hat{x}_{m,0}$ , there always exists a time instant  $i_0$  such that

$$\hat{x}_{m,i_0} < 0, \quad \forall m = 1, \dots, M-1. \quad (109)$$

The recursion  $\hat{x}_{m,i} = F_m(\hat{x}_{m,i-1}) - \beta d_m$  exhibits the following properties:

- If  $\hat{x}_{m,i-1} < 0$ ,

$$\hat{x}_{m,i-1} - \beta d_m < \hat{x}_{m,i} < -\beta d_m, \quad (110)$$

- If  $\hat{x}_{m,i-1} \geq 0$ ,

$$-\beta d_m \leq \hat{x}_{m,i} \leq \hat{x}_{m,i-1} - \beta d_m. \quad (111)$$

From (110) and (111), if  $\hat{x}_{m,0} \geq 0$ ,  $\hat{x}_{m,i}$  will decrease in each recursion by subtracting  $\beta d_m$  until it becomes less than 0, and it will remain less than 0 thereafter. Taking

$$i_0 \geq \max_{m=1, \dots, M-1} \left\{ \frac{\hat{x}_{m,0}}{\beta d_m} + 1, 0 \right\}, \quad (112)$$

ensures that (109) is satisfied. Additionally, when  $\hat{x}_{m,i-1} \geq 0 > \hat{x}_m^\infty$  (which also implies that  $\hat{x}_{m,0} \geq 0$ ), we have:

$$\hat{x}_{m,i} \geq -\beta d_m \geq \hat{x}_m^\infty. \quad (113)$$

Thus:

$$\begin{aligned} |\hat{x}_{m,i} - \hat{x}_m^\infty| &= \hat{x}_{m,i} - \hat{x}_m^\infty \\ &\leq \hat{x}_{m,i-1} - \beta d_m - \hat{x}_m^\infty \\ &= \left( 1 - \frac{\beta d_m}{\hat{x}_{m,i-1} - \hat{x}_m^\infty} \right) (\hat{x}_{m,i-1} - \hat{x}_m^\infty) \\ &\stackrel{(a)}{\leq} \frac{\hat{x}_{m,0} - \log \frac{\alpha}{1-\alpha M + \alpha}}{\hat{x}_{m,0} - \log \frac{\alpha}{1-\alpha M + \alpha} + \beta d_m} (\hat{x}_{m,i-1} - \hat{x}_m^\infty) \\ &\leq \frac{\bar{x}_0 - \log \frac{\alpha}{1-\alpha M + \alpha}}{\bar{x}_0 - \log \frac{\alpha}{1-\alpha M + \alpha} + \beta \underline{d}} (\hat{x}_{m,i-1} - \hat{x}_m^\infty) \\ &= \frac{\bar{x}_0 - \log \frac{\alpha}{1-\alpha M + \alpha}}{\bar{x}_0 - \log \frac{\alpha}{1-\alpha M + \alpha} + \beta \underline{d}} |\hat{x}_{m,i-1} - \hat{x}_m^\infty|. \end{aligned} \quad (114)$$

Here, step (a) holds since

$$\hat{x}_{m,i} \leq \hat{x}_{m,0} - i\beta d_m \leq \hat{x}_{m,0}, \quad (115)$$

and by Lemma 2:

$$\begin{aligned} \hat{x}_m^\infty &\geq \log \frac{\alpha}{\alpha \exp(\beta d_m) + (1 - \alpha M)(\exp(\beta d_m) - 1)} \\ &\geq \log \frac{\alpha}{(1 - \alpha M + \alpha) \exp(\beta d_m)} \\ &= \log \frac{\alpha}{1 - \alpha M + \alpha} - \beta d_m \end{aligned} \quad (116)$$

Next, we invoke the following lemma to complete the proof:

*Lemma 4 (Banach Fixed Point Theorem [31]):* If

$T : X \rightarrow X$  is a contraction on a complete metric space  $(X, \rho)$ , then there is a unique fixed point  $x \in X$  (35).

Starting from  $i_0$ , the sequence  $\hat{x}_i$  will always remain within  $(-\infty, 0]^{M-1}$ . Therefore, by Lemma 1 and Lemma 4, there exists a unique fixed point  $\hat{x}^\infty \in (-\infty, 0]^{M-1}$ , such that

$$\lim_{i \rightarrow \infty} \hat{x}_i = \hat{x}^\infty. \quad (117)$$

From the proof of Lemma 1, when  $\hat{x}_{m,i-1} \leq 0$ :

$$\begin{aligned} |\hat{x}_{m,i} - \hat{x}_m^\infty| &= |F_m(\hat{x}_{m,i-1}) - F_m(\hat{x}^\infty)| \\ &= \left| \sum_{\ell=1}^{M-1} [J_F(c_{i-1})]_{m\ell} (\hat{x}_{\ell,i-1} - \hat{x}_\ell^\infty) \right| \\ &\stackrel{(b)}{\leq} \left( \sum_{\ell=1}^{M-1} [J_F(c_{i-1})]_{m\ell} \right) \|\hat{x}_{i-1} - \hat{x}^\infty\|_\infty \\ &\stackrel{(105)}{\leq} \frac{1 - \alpha M}{1 - \alpha M + 2\alpha} \|\hat{x}_{i-1} - \hat{x}^\infty\|_\infty. \end{aligned} \quad (118)$$

Here  $c_{i-1} = t\hat{x}_{i-1} + (1-t)\hat{x}^\infty$  with  $t \in (0, 1)$ , and step (b) holds since  $c_{m,i-1} \leq 0$  and from the proof of Lemma 1,

$$[J_F(c_{i-1})]_{m\ell} \geq 0, \quad 1 \leq m, \ell \leq M-1. \quad (119)$$

Combining (114) and (118) together, we conclude that (42) holds.

**APPENDIX III**  
**PROOF OF THEOREM 2**

From Lemma 2, for all  $m = 1, \dots, M-1$ , we have

$$\exp(\hat{x}_m^\infty) = \frac{\alpha}{\alpha \exp(\beta d_m) + (1 - \alpha M)(\exp(\beta d_m) - 1) \hat{\mu}_0^\infty}, \quad (120)$$

which leads to

$$\begin{aligned} \alpha \exp(\beta d_m) \exp(\hat{x}_m^\infty) \\ + (\exp(\beta d_m) - 1)(1 - \alpha M) \hat{\mu}_0^\infty \exp(\hat{x}_m^\infty) = \alpha. \end{aligned} \quad (121)$$

Summing over  $m = 1, \dots, M-1$ , we have:

$$\begin{aligned} \alpha(M-1) \\ = ((1 - \alpha M) \hat{\mu}_0^\infty + \alpha) \sum_{m=1}^{M-1} \exp(\hat{x}_m^\infty) \exp(\beta d_m) \\ - (1 - \alpha M) \hat{\mu}_0^\infty \sum_{m=1}^{M-1} \exp(\hat{x}_m^\infty). \end{aligned} \quad (122)$$

Using (73),  $\sum_{m=1}^{M-1} \exp(\hat{x}_m^\infty) = 1/\hat{\mu}_0^\infty - 1$ , we obtain:

$$\begin{aligned} 1 - \alpha - (1 - \alpha M) \hat{\mu}_0^\infty \\ = ((1 - \alpha M) \hat{\mu}_0^\infty + \alpha) \sum_{m=1}^{M-1} \exp(\beta d_m) \exp(\hat{x}_m^\infty) \\ \geq ((1 - \alpha M) \hat{\mu}_0^\infty + \alpha) \exp(\beta \underline{d}) (1/\hat{\mu}_0^\infty - 1). \end{aligned} \quad (123)$$

Since  $\hat{\mu}_0^\infty < 1$ , we have

$$1 - \alpha > (1 - \alpha M) \exp(\beta \underline{d}) - (1 - \alpha M)(\exp(\beta \underline{d}) - 1) \hat{\mu}_0^\infty. \quad (124)$$

With  $1 - \alpha M > 0$  and  $\exp(\underline{d}) > 1$  from Assumption 2, this inequality establishes the lower bound:

$$\hat{\mu}_0^\infty > \frac{(1 - \alpha M) \exp(\beta \underline{d}) - 1 + \alpha}{(1 - \alpha M)(\exp(\beta \underline{d}) - 1)} = \underline{\mu}. \quad (125)$$

On the other hand, we also have

$$\begin{aligned} 1 - \alpha - (1 - \alpha M) \hat{\mu}_0^\infty \\ \leq ((1 - \alpha M) \hat{\mu}_0^\infty + \alpha) \exp(\beta \bar{d}) (1/\hat{\mu}_0^\infty - 1), \end{aligned} \quad (126)$$

Using the previously derived lower bound for  $\hat{\mu}_0^\infty$ , the upper bound can be similarly obtained:

$$\hat{\mu}_0^\infty < \frac{(1 - \alpha M - \alpha + \alpha/\underline{\mu}) \exp(\beta \bar{d}) - 1 + \alpha}{(1 - \alpha M)(\exp(\beta \bar{d}) - 1)}. \quad (127)$$

This completes the proof.

#### APPENDIX IV PROOF OF LEMMA 3

We first show that, under Assumption 3 and the dynamics in (80), the log-belief ratio can be bounded almost surely.

*Lemma 5:* The log-belief ratio  $\mathbf{x}_{m,i}$  in (80) satisfies:

$$q_m \leq \mathbf{x}_{m,i} \leq Q_m \quad a.s., \quad (128)$$

where

$$q_m = \log \frac{\alpha}{1 - \alpha M + \alpha} - \beta d_m - \beta C, \quad (129)$$

$$Q_m = \log \frac{1 - \alpha M + \alpha}{\alpha} - \beta d_m + \beta C. \quad (130)$$

$C$  is defined as in (78).

*Proof:* Supplementary Material III. ■

Define  $\delta_{m,i} = \log \frac{L(\xi_i|\theta_m)}{L(\xi_i|\theta_0)} + d_m$ . Then, the original and reference dynamics can be expressed as:

$$\mathbf{x}_{m,i} = F_m(\mathbf{x}_{1,i-1}, \dots, \mathbf{x}_{M-1,i-1}) - \beta d_m + \beta \delta_{m,i}, \quad (131)$$

and

$$\hat{\mathbf{x}}_{m,i} = F_m(\hat{\mathbf{x}}_{1,i-1}, \dots, \hat{\mathbf{x}}_{M-1,i-1}) - \beta d_m. \quad (132)$$

For any  $x$ , if  $0 \leq x_m \leq Q_m$ , notice that  $F_m(\hat{\mathbf{x}}^\infty) - \beta d_m = \hat{\mathbf{x}}_m^\infty$ , we have:

$$\begin{aligned} & |F_m(x) - F_m(\hat{\mathbf{x}}^\infty)| \\ &= F_m(x) - F_m(\hat{\mathbf{x}}^\infty) \\ &\leq x_m - \beta d_m - \hat{\mathbf{x}}_m^\infty \\ &\leq \left(1 - \frac{\beta d_m}{x_m - \hat{\mathbf{x}}_m^\infty}\right) (x_m - \hat{\mathbf{x}}_m^\infty) \\ &\stackrel{(a)}{\leq} \left(1 - \frac{\beta d_m}{2 \log \frac{1 - \alpha M + \alpha}{\alpha} + \beta C}\right) (x_m - \hat{\mathbf{x}}_m^\infty) \\ &\leq \left(1 - \frac{\beta \underline{d}}{2 \log \frac{1 - \alpha M + \alpha}{\alpha} + \beta C}\right) |x_m - \hat{\mathbf{x}}_m^\infty|, \end{aligned} \quad (133)$$

here step (a) follows from Lemma 5 and (116).

If  $q_m \leq x_m < 0$ , then from Lemma 1:

$$\begin{aligned} |F_m(x) - F_m(\hat{\mathbf{x}}^\infty)| &= \left| \sum_{\ell=1}^{M-1} [J_F(c)]_{m\ell} (x_\ell - \hat{\mathbf{x}}_\ell^\infty) \right| \\ &\stackrel{(a)}{\leq} \left( \sum_{\ell=1}^{M-1} [J_F(c)]_{m\ell} \right) \|x - \hat{\mathbf{x}}^\infty\|_\infty \\ &\stackrel{(105)}{\leq} \frac{1 - \alpha M}{1 - \alpha M + 2\alpha} \|x - \hat{\mathbf{x}}^\infty\|_\infty. \end{aligned} \quad (134)$$

Here  $c = tx + (1-t)\hat{\mathbf{x}}^\infty$  with  $t \in (0, 1)$ , and step (a) holds since  $c_m < 0$  and from the proof of Lemma 1,

$$[J_F(c)]_{m\ell} > 0, \quad 1 \leq m, \ell \leq M-1. \quad (135)$$

Let  $Q = \max_{m=1, \dots, M-1} \{|Q_m|, |q_m|\}$ , for all  $x \in [-Q, Q]^{M-1}$  we have:

$$\|F(x) - F(\hat{\mathbf{x}}^\infty)\|_\infty \leq \lambda_1 \|x - \hat{\mathbf{x}}^\infty\|_\infty, \quad (136)$$

where  $\lambda_1$  is as defined in (83).

From the recursion (131) and (132), we have:

$$\begin{aligned} & \mathbb{E} [\|\mathbf{x}_i - \hat{\mathbf{x}}^\infty\|_\infty | \mathbf{x}_{i-1}] \\ &= \mathbb{E} [\|F(\mathbf{x}_{i-1}) - F(\hat{\mathbf{x}}^\infty) + \beta \delta_i\|_\infty | \mathbf{x}_{i-1}] \\ &\leq \mathbb{E} [\|F(\mathbf{x}_{i-1}) - F(\hat{\mathbf{x}}^\infty)\|_\infty | \mathbf{x}_{i-1}] + \beta \mathbb{E} [\|\delta_i\|_\infty] \\ &\stackrel{(b)}{\leq} \lambda_1 \mathbb{E} [\|\mathbf{x}_{i-1} - \hat{\mathbf{x}}^\infty\|_\infty | \mathbf{x}_{i-1}] + \beta C. \end{aligned} \quad (137)$$

Here step (b) is due to (136) along with Assumption 3.

By taking expectation again, we obtain

$$\begin{aligned} & \mathbb{E} [\|\mathbf{x}_i - \hat{\mathbf{x}}^\infty\|_\infty] \\ &\leq \lambda_1 \mathbb{E} [\|\mathbf{x}_{i-1} - \hat{\mathbf{x}}^\infty\|_\infty] + \beta C \\ &\leq \lambda_1^i \mathbb{E} [\|\mathbf{x}_0 - \hat{\mathbf{x}}^\infty\|_\infty] + \frac{\beta C(1 - \lambda_1^i)}{1 - \lambda_1} \\ &\leq O(\lambda_1^i) + \frac{\beta C}{1 - \lambda_1}. \end{aligned} \quad (138)$$

#### APPENDIX V PROOF OF THEOREM 3

The instantaneous error probability can be computed as:

$$\begin{aligned} p_i^e &= \mathbb{P} [\exists \theta_m \neq \theta_0, \text{ s.t. } \boldsymbol{\mu}_i(\theta_m) \geq \boldsymbol{\mu}_i(\theta_0)] \\ &= \mathbb{P} [\exists \theta_m \neq \theta_0, \text{ s.t. } \mathbf{x}_{m,i} \geq 0] \\ &\leq \mathbb{P} [\exists \theta_m \neq \theta_0, \text{ s.t. } \mathbf{x}_{m,i} - \hat{\mathbf{x}}_m^\infty \geq -\bar{x}^\infty] \\ &\leq \mathbb{P} \left[ \max_{m=1, \dots, M-1} |\mathbf{x}_{m,i} - \hat{\mathbf{x}}_m^\infty| \geq -\bar{x}^\infty \right] \\ &= \mathbb{P} [\|\mathbf{x}_i - \hat{\mathbf{x}}^\infty\|_\infty \geq -\bar{x}^\infty] \\ &\stackrel{(a)}{\leq} \frac{\mathbb{E} [\|\mathbf{x}_i - \hat{\mathbf{x}}^\infty\|_\infty]}{-\bar{x}^\infty} \\ &\stackrel{(b)}{\leq} \frac{O(\lambda_1^i) + \beta C}{-(1 - \lambda_1)\bar{x}^\infty}. \end{aligned} \quad (139)$$

where step (a) is due to Markov's inequality and step (b) follows from Lemma 3.

Furthermore, due to the fact that:

$$\lambda_1 < 1, \quad (140)$$

we always have:

$$\limsup_{i \rightarrow \infty} p_i^e \leq \frac{\beta C}{-(1 - \lambda_1)\bar{x}^\infty}. \quad (141)$$

If  $\alpha \rightarrow 0$ , we have:

$$\frac{\beta \underline{d}}{2 \log \frac{1 - \alpha M + \alpha}{\alpha} + \beta C} = O\left(\frac{1}{\log \alpha}\right), \quad (142)$$

thus

$$1 - \lambda_1 = \min \left\{ \frac{2\alpha}{1 - \alpha M + 2\alpha}, \frac{\beta \underline{d}}{2 \log \frac{1 - \alpha M + \alpha}{\alpha} + \beta C} \right\} = O(\alpha). \quad (143)$$

Moreover, from (74) and (37), we have:

$$\lim_{\alpha \rightarrow 0} \hat{\mu}_0^\infty = 1, \quad (144)$$

and then for all  $m = 1, \dots, M - 1$ ,

$$\lim_{\alpha \rightarrow 0} \hat{x}_m^\infty = -\infty. \quad (145)$$

If  $\beta = O(\alpha)$ , then:

$$\lim_{\alpha \rightarrow 0} \left( \limsup_{i \rightarrow \infty} p_i^e \right) \leq \frac{\beta C}{-(1 - \lambda_1) \bar{x}^\infty} = \frac{O(1)}{-\bar{x}^\infty} = 0. \quad (146)$$

On the other hand, as  $p_i^e$  is a probability measure, it is obvious that:

$$\lim_{\alpha \rightarrow 0} \left( \limsup_{i \rightarrow \infty} p_i^e \right) \geq 0. \quad (147)$$

By applying the squeeze theorem for limits, we then have:

$$\lim_{\alpha \rightarrow 0} \left( \limsup_{i \rightarrow \infty} p_i^e \right) = 0. \quad (148)$$

## REFERENCES

- [1] M. Thomas and A. T. Joy, *Elements of information theory*. Wiley-Interscience, 2006.
- [2] A. V. Banerjee, "A simple model of herd behavior," *The quarterly journal of economics*, vol. 107, no. 3, pp. 797–817, 1992.
- [3] S. Bikhchandani, D. Hirshleifer, and I. Welch, "A theory of fads, fashion, custom, and cultural change as informational cascades," *Journal of political Economy*, vol. 100, no. 5, pp. 992–1026, 1992.
- [4] D. Acemoglu, M. A. Dahleh, I. Lobel, and A. Ozdaglar, "Bayesian learning in social networks," *The Review of Economic Studies*, vol. 78, no. 4, pp. 1201–1236, 2011.
- [5] A. Jadbabaie, P. Molavi, A. Sandroni, and A. Tahbaz-Salehi, "Non-bayesian social learning," *Games and Economic Behavior*, vol. 76, no. 1, pp. 210–225, 2012.
- [6] P. Molavi, A. Tahbaz-Salehi, and A. Jadbabaie, "A theory of non-bayesian social learning," *Econometrica*, vol. 86, no. 2, pp. 445–490, 2018.
- [7] A. Nedić, A. Olshevsky, and C. A. Uribe, "Fast convergence rates for distributed non-bayesian learning," *IEEE Transactions on Automatic Control*, vol. 62, no. 11, pp. 5538–5553, 2017.
- [8] A. Lalitha, T. Javidi, and A. D. Sarwate, "Social learning and distributed hypothesis testing," *IEEE Transactions on Information Theory*, vol. 64, no. 9, pp. 6161–6179, 2018.
- [9] V. Bordinon, S. Vlaski, V. Matta, and A. H. Sayed, "Learning from heterogeneous data based on social interactions over graphs," *IEEE Transactions on Information Theory*, vol. 69, no. 5, pp. 3347–3371, 2022.
- [10] B. Wu and C. A. Uribe, "Frequentist guarantees of distributed (non)-bayesian inference," *arXiv preprint arXiv:2311.08214*, 2023.
- [11] C. Chamley, *Rational herds: Economic models of social learning*. Cambridge University Press, 2004.
- [12] D. Acemoglu and A. Ozdaglar, "Opinion dynamics and learning in social networks," *Dynamic Games and Applications*, vol. 1, pp. 3–49, 2011.
- [13] B. D. Anderson and J. B. Moore, *Optimal filtering*. Courier Corporation, 2005.
- [14] V. Krishnamurthy, "Optimal filtering," in *Partially observed Markov decision processes*. Cambridge university press, 2016, ch. 3, pp. 57–59.
- [15] L. E. Baum and T. Petrie, "Statistical inference for probabilistic functions of finite state markov chains," *The annals of mathematical statistics*, vol. 37, no. 6, pp. 1554–1563, 1966.
- [16] B. Mor, S. Garhwal, and A. Kumar, "A systematic review of hidden markov models and their applications," *Archives of computational methods in engineering*, vol. 28, pp. 1429–1448, 2021.
- [17] L. R. Rabiner, S. E. Levinson, and M. M. Sondhi, "On the application of vector quantization and hidden markov models to speaker-independent, isolated word recognition," *Bell System Technical Journal*, vol. 62, no. 4, pp. 1075–1105, 1983.
- [18] L. R. Rabiner, "A tutorial on hidden markov models and selected applications in speech recognition," *Proceedings of the IEEE*, vol. 77, no. 2, pp. 257–286, 1989.
- [19] M. Gales, S. Young *et al.*, "The application of hidden markov models in speech recognition," *Foundations and Trends® in Signal Processing*, vol. 1, no. 3, pp. 195–304, 2008.
- [20] J. Yamato, J. Ohya, and K. Ishii, "Recognizing human action in time-sequential images using hidden markov model." in *CVPR*, vol. 92, 1992, pp. 379–385.
- [21] J. Yang, Y. Xu, and C. S. Chen, "Human action learning via hidden markov model," *IEEE Transactions on Systems, Man, and Cybernetics-Part A: Systems and Humans*, vol. 27, no. 1, pp. 34–44, 1997.
- [22] P. Asghari, E. Soleimani, and E. Nazerfard, "Online human activity recognition employing hierarchical hidden markov models," *Journal of Ambient Intelligence and Humanized Computing*, vol. 11, pp. 1141–1152, 2020.
- [23] E. Birney, "Hidden markov models in biological sequence analysis," *IBM journal of Research and Development*, vol. 45, no. 3.4, pp. 449–454, 2001.
- [24] P. Chigansky, R. Liptser, and R. Van Handel, "Intrinsic methods in filter stability," *Handbook of Nonlinear Filtering*, 2009.
- [25] L. Shue, D. Anderson, and S. Dey, "Exponential stability of filters and smoothers for hidden markov models," *IEEE Transactions on Signal Processing*, vol. 46, no. 8, pp. 2180–2194, 1998.
- [26] C. McDonald and S. Yüksel, "Exponential filter stability via dobrushin's coefficient," *Electronic Communications in Probability*, 2020.
- [27] —, "Stability of non-linear filters and observability of stochastic dynamical systems," *arXiv preprint arXiv:1812.01772*, 2018.
- [28] V. Bordinon, V. Matta, and A. H. Sayed, "Adaptive social learning," *IEEE Transactions on Information Theory*, vol. 67, no. 9, pp. 6053–6081, 2021.
- [29] M. Kayaalp, V. Bordinon, S. Vlaski, V. Matta, and A. H. Sayed, "Distributed bayesian learning of dynamic states," *arXiv preprint arXiv:2212.02565*, 2022.
- [30] M. Khammassi, V. Bordinon, V. Matta, and A. H. Sayed, "Adaptive social learning for tracking rare transition markov chains," in *2024 32nd European Signal Processing Conference (EUSIPCO)*, 2024, pp. 1032–1036.
- [31] J. K. Hunter and B. Nachtergaele, "The contraction mapping theorem," in *Applied analysis*. World Scientific Publishing Company, 2001, ch. 3, pp. 61–63.